

NASA Technical Paper 1117

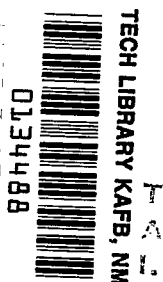
Tensile Stress-Strain Behavior
of Boron/Aluminum Laminates

J. A. Sova and C. C. Poe, Jr.

FEBRUARY 1978

NASA

LOAN COPY: F
AFWL TECHNICAL
KIRTLAND AF





NASA Technical Paper 1117

Tensile Stress-Strain Behavior of Boron/Aluminum Laminates

J. A. Sova

The George Washington University
Joint Institute for Advancement of Flight Sciences
Langley Research Center
Hampton, Virginia

and

C. C. Poe, Jr.

Langley Research Center
Hampton, Virginia



National Aeronautics
and Space Administration

**Scientific and Technical
Information Office**

1978

SUMMARY

The tensile stress-strain behavior of five types of boron/aluminum laminates was investigated. Two of the laminate types contained only 0° or 45° fibers ($[0]_{6T}$ and $[\pm 45]_{2S}$); the remaining three consisted of both 0° and 45° plies ($[0/\pm 45]_S$, $[0_2/\pm 45]_S$, and $[\pm 45/0_2]_S$). Longitudinal and transverse stress-strain curves were obtained for monotonic loading to failure and for three cycles of loading to successively higher load levels.

For the laminates with 0° plies in the loading direction, the ultimate strengths varied linearly with the percentage of 0° plies in the composite. The strengths predicted by assuming that the 0° plies failed first correlated well with the experimental results. The stress-strain curves for all the boron/aluminum laminates were nonlinear except at very small strains. Within the small linear regions, elastic constants calculated from laminate theory corresponded to those obtained experimentally to within 10 to 20 percent. However, because of the nonlinearity, the elastic constants do not characterize the laminates over a significant part of their working range. The nonlinearity in the stress-strain curves was greater at higher percentages of 45° plies in the laminate.

A limited amount of cyclic loading did not affect the ultimate strength and strain for the boron/aluminum laminates. The laminates, however, exhibited a permanent strain on unloading. As with the nonlinearity in the stress-strain curves, the amount of permanent strain was greater for laminates with more 45° plies.

The Ramberg-Osgood equation was fitted to the stress-strain curves to obtain average curves for the various laminates. The equation fitted the experimental data well.

INTRODUCTION

The analysis of structures made from boron/aluminum laminates is complicated by the inelasticity and nonlinearity of the stress-strain behavior in the working range of the material. Although the mechanical properties of boron/aluminum laminates have been studied (see, for example, refs. 1, 2, and 3), the stress-strain behavior has not been adequately characterized.

The objective of this investigation was to characterize the stress-strain behavior of several types of boron/aluminum laminates. Two of the laminate types consisted of only 0° or 45° plies; three other laminate types contained both 0° and 45° plies. Both longitudinal and transverse stress-strain curves were obtained for the various laminates. To investigate the inelasticity of the material, some specimens were also subjected to a few loading cycles. The

Ramberg-Osgood equation was fitted to the experimental stress-strain data. Elastic constants and the extent of the linear regions in the stress-strain curves were determined for the various laminates. Elastic constants calculated from laminate theory were compared with measured values.

SYMBOLS

Although values are given in the International System of Units (SI) in this report, the experimental procedures were carried out using U.S. Customary Units.

b	constant in the Ramberg-Osgood equation, Pa^{-1}
E	Young's modulus of elasticity, Pa
E_f	Young's modulus of elasticity of fibers, Pa
E_s	secondary modulus, Pa
E_{tan}	tangent modulus, Pa
F_{tu}	ultimate tensile strength, Pa
G_{12}	lamina shear modulus, Pa
G_{xy}	laminate shear modulus, Pa
g	acceleration due to gravity, m/sec^2
n	constant in the Ramberg-Osgood equation
V_f	fiber volume fraction
Γ	percentage of 45° plies
γ	shear strain
ϵ	axial strain
ϵ_{tu}	ultimate tensile strain
Λ	percentage of plies with fibers in loading direction
ν	Poisson's ratio
ν_{tan}	tangent Poisson's ratio
σ	axial stress, Pa
σ_ϵ	axial stress at a strain of ϵ , Pa

τ shear stress, Pa

Subscripts:

x, y Cartesian coordinates

α, β, η, ξ refer to legs of strain gage rosettes (see fig. 2)

The notation for laminate orientation used in reference 4 is used in the present report. The cross-ply angles are listed in the order of layup, separated by a slash, with the entire listing enclosed within brackets. Where there is more than one consecutive lamina at any given angle, the number of laminae at that angle is denoted by a numerical subscript within the brackets. Subscript S outside the brackets denotes symmetric; for example, $[0/\pm 45]_S$

means $[0/+45/-45/-45/+45/0]$. Subscript T outside the brackets denotes total; for example, $[0]_{6T}$ means $[0/0/0/0/0/0]$.

EXPERIMENTAL PROCEDURES

Material and Specimens

A diffusion-bonded boron/aluminum sheet material consisting of 0.142-mm-diameter boron fibers embedded in 6061 aluminum matrix was used in this investigation. The material, which was fabricated for a larger fracture program, was tested in the "as fabricated" condition. Ultrasonic (C-scan) inspection did not reveal any voids in the material. As shown in the following table, 60 sheets of the material, which included 5 types of laminates were used. The sheets were delivered in two sizes: 508 by 457 mm and 508 by 305 mm. The 0° fiber direction was parallel to the 508-mm sides. (See fig. 1.) The fiber volume fraction, specified to be 45 to 50 percent, was higher for the unidirectional laminates than for the laminates with cross plies, as indicated in the table. The average sheet thickness listed in the table was calculated by averaging measured thicknesses of all the sheets of a single laminate orientation.

Sheet number	Laminate orientation	Average sheet thickness, mm	Number of plies	Average ply thickness, mm	Volume fraction, percent
1 to 10	$[0]_{6T}$	1.068	6	0.178	50
11 to 25	$[+45]_{2S}$	1.528	8	.191	45
26 to 40	$[0/\pm 45]_S$	1.110	6	.185	45
41 to 55	$[0_2/\pm 45]_S$	1.488	8	.186	44
56 to 60	$[+45/0_2]_S$	1.512	8	.189	44

One longitudinal and one transverse tensile specimen were tested from each sheet of material. (See fig. 1.) The specimens were of simple rectangular shape, 19.0 mm wide and 254.0 mm long, and were numbered according to the following four-digit system: the first two digits denote the sheet number, the third digit denotes the position of the specimen within the original sheet, and the fourth digit indicates whether the specimen was longitudinal or transverse.

Test Procedure and Equipment

The specimens were tested in a hydraulically actuated, closed-loop, servo-controlled testing machine with hydraulic grips. Plastic tabs about 3 mm thick were placed between the grips and the specimens to protect the surface of the specimens. Radiographs showed that the gripping pressure necessary to hold the specimens did not damage the boron fibers. No specimens failed in the grips.

Loads for the static tensile tests were programmed by an analog ramp generator to vary linearly with time. The specimens were loaded to failure slowly (in about 2 minutes) so that at least 50 load-strain readings could be recorded during each test.

For the cyclic tensile tests, the specimens were loaded to 0.267 of the static ultimate strength, unloaded, reloaded to 0.467 of the ultimate strength, unloaded, reloaded to 0.667 of the ultimate strength, unloaded, and finally loaded to failure. The values of 0.267 and 0.667 of the ultimate strength represent the upper values of a 1g load (transport-type airplane) and of a limit load, respectively; 0.467 of the ultimate strength is the average of the other two values.

Strain gage rosettes were used to measure strains in the direction of load and at angles of $\pm 45^\circ$ to the load direction. The gages were bonded to the center of the specimens on both front and back sides. The transverse and shear strains for each rosette were calculated from the measured strains as follows:

$$\left. \begin{aligned} \epsilon_\eta &= \epsilon_\alpha + \epsilon_\beta - \epsilon_\xi \\ \gamma &= \epsilon_\alpha - \epsilon_\beta \end{aligned} \right\} \quad (1)$$

where the subscripts refer to the legs of the rosette shown in figure 2. The axial and shear strains on both sides of each specimen were averaged to eliminate any strains due to bending in the specimens. The shear strains were very small compared with the axial strains, indicating that the loads were applied without twist or shear.

During both the static and cyclic tests, the output signals from the strain gages, the load cell, and a peak-load reader were recorded on the digital data acquisition system shown schematically in figure 3. As shown in figure 2, the output signals were recorded on 12 channels, and the load was recorded 4 times during each scan. These analog output signals were scanned continuously at about 2 seconds per scan, were converted into digital signals, and then were printed on paper tape and recorded on magnetic tape. The scan number, the specimen number, and the time to the nearest second were also

recorded. Subsequently, the data on the magnetic tapes were analyzed by a digital computer. The maximum load used to calculate the ultimate tensile strength was determined from the peak-load reader.

Because the load varied while the strains were recorded, the computer program used the following procedure to derive the stress-strain curves. The load corresponding to a recorded strain was calculated by linearly interpolating between loads recorded before and after the particular strain. The linear interpolation was quite accurate because the load varied linearly with time and the scanning rate was constant. The average sheet thickness for a particular laminate orientation was used to calculate the corresponding stresses.

In calculating ϵ_η and γ by equations (1), ϵ_α and ϵ_β corresponding to ϵ_ξ were calculated by linearly interpolating between values of ϵ_α and ϵ_β recorded before and after ϵ_ξ . Because of the nonlinear response of the material, the strains did not vary linearly with time as did the loads. Nevertheless, the linear interpolation was quite accurate because the change in strain was very small between recordings.

STRESS-STRAIN RELATIONSHIP

Assuming the boron/aluminum laminates to be homogeneous materials with orthotropic properties and in a state of plane stress, the linear strain-stress relations are (ref. 5)

$$\epsilon_y = \frac{\sigma_y}{E_y} - \frac{\sigma_x \nu_{xy}}{E_x} \quad (2)$$

$$\epsilon_x = \frac{\sigma_x}{E_x} - \frac{\sigma_y \nu_{yx}}{E_y} \quad (3)$$

$$\gamma_{yx} = \frac{\tau_{yx}}{G_{yx}} \quad (4)$$

The laminate principal axes are referred to as y and x in this report, the y-direction always being the direction of the 0° fibers. Four independent elastic constants present in equations (2) to (4) characterize the laminates: Young's moduli in the y- and x-directions, E_y and E_x ; the shear modulus G_{yx} ; and the major Poisson's ratio ν_{yx} . The fifth elastic constant, ν_{xy} , is related to the other constants as follows:

$$\nu_{xy} E_y = \nu_{yx} E_x \quad (5)$$

The following form of the well-known Ramberg-Osgood equation (ref. 6) was chosen to represent the tensile stress-strain curves of the boron/aluminum material:

$$\epsilon = \frac{\sigma}{E} + (b\sigma)^n \quad (6)$$

For orthotropic laminates, equation (6) can be written as follows for ϵ_y and ϵ_x : for uniaxial loading in the y-direction,

$$\left. \begin{aligned} \epsilon_y &= \frac{\sigma_y}{E_y} + (b_{yy}\sigma_y)^{n_{yy}} \\ \epsilon_x &= -\frac{\sigma_y \nu_{yx}}{E_y} - (b_{yx}\sigma_y)^{n_{yx}} \end{aligned} \right\} \quad (7)$$

and for uniaxial loading in the x-direction,

$$\left. \begin{aligned} \epsilon_y &= -\frac{\sigma_x \nu_{xy}}{E_x} - (b_{xy}\sigma_x)^{n_{xy}} \\ \epsilon_x &= \frac{\sigma_x}{E_x} + (b_{xx}\sigma_x)^{n_{xx}} \end{aligned} \right\} \quad (8)$$

Equations (7) were fitted to stress-strain data for longitudinal specimens and equations (8) to data for transverse specimens. For linear-elastic behavior, the nonlinear term in equation (6) is zero, and equations (7) and (8) reduce to the uniaxial loading forms of equations (2) and (3). Note that because the constants in the nonlinear terms in equations (7) and (8) were derived from uniaxial tests, the sum of the equations may not give correct strains for biaxially applied stresses. The elastic constants E and ν were calculated using only the linear-elastic part of the stress-strain curves, and the constants b and n were calculated using all of each curve. The procedure is given in the appendix.

RESULTS AND DISCUSSION

Static Tensile Tests

Stress-strain curves.— Stress-strain curves for the static tensile tests are presented in figures 4 to 8 for each laminate orientation. Each figure shows the measured strains in the y- and x-directions and average Ramberg-Osgood curves. The results for longitudinal and transverse specimens are shown in separate graphs in each figure. Note that for laminates containing 0° fibers, the stress scales for longitudinal and transverse tests in parts (a) and (b) of the figures differ by as much as a factor of 10. In general, the stress-strain curves are very nonlinear, and the Ramberg-Osgood curves model the experimental ones well. The curves are shown to failure except for the $[\pm 45]_{2S}$ laminates where the strain gages debonded before failure. Tables I

to V present various parameters measured in the tests or calculated from the data, including the Ramberg-Osgood constants.

Figure 9 shows average Ramberg-Osgood stress-strain curves for all the laminates. The ultimate tensile strains of the four laminates with fibers in the direction of loading are about the same, 0.007 to 0.008. (See fig. 9(a).) In transverse tests of the four laminates, with some fibers normal to the loading direction, the ultimate tensile strains were much smaller and varied greatly, 0.0020 to 0.0065. For the $[\pm 45]_{2S}$ laminate orientations, the ultimate tensile strains were much higher than the 0.02 to 0.03 at which the gages failed; the ultimate strain given by the average Ramberg-Osgood equation for the average measured ultimate stress of 220.6 MPa is 0.05.

The stress-strain data show that the degree of nonlinearity is greater for higher proportions of 45° plies. In order to examine the nonlinearity in more detail, the tangent moduli and Poisson's ratios were calculated for both the test data and the average Ramberg-Osgood curves. The tangent moduli are given by

$$\left. \begin{aligned} (E_{\text{tan}})_x &= \frac{\partial \sigma_x}{\partial \epsilon_x} \\ (E_{\text{tan}})_y &= \frac{\partial \sigma_y}{\partial \epsilon_y} \end{aligned} \right\} \quad (9)$$

and Poisson's ratios by

$$\left. \begin{aligned} (\nu_{\text{tan}})_{yx} &= - \frac{\partial \epsilon_x}{\partial \epsilon_y} \\ (\nu_{\text{tan}})_{xy} &= - \frac{\partial \epsilon_y}{\partial \epsilon_x} \end{aligned} \right\} \quad (10)$$

The derivatives in equations (9) and (10) were calculated for the test data by taking the ratio of changes in stress and strain between successive readings.

Figures 10 to 14 show the applied stress plotted against the tangent modulus and Poisson's ratio for each laminate orientation. For laminates with some fibers in the loading direction, the curves for tangent modulus show that the laminates yielded at very low stresses, and the modulus approached a secondary value lower than the initial tangent modulus. If the laminate contained no fibers in the loading direction, the tangent modulus approached zero for high stresses. The low yield strength of the composite is due to the low yield strength of the aluminum matrix. With some fibers in the loading direction, the tangent moduli at high stresses agree well with those calculated by the following equation which assumes that the fibers in the loading direction carry all the load:

$$E_s = \frac{V_f E_f \Lambda}{100} \quad (11)$$

where Λ equals the percentage of plies with fibers in the loading direction. Values of $V_f = 0.5$ and $E_f = 400$ GPa were used for the volume fraction and fiber modulus, respectively.

As previously noted, the overall conformity between the experimental stress-strain data and the approximating Ramberg-Osgood curves is good. However, figures 10 to 14 show that for laminates loaded in the direction of 0° fibers, the shape of the tangent modulus curve given by the Ramberg-Osgood equation does not agree well with the data for large stresses, because the equation does not asymptotically approach a secondary modulus for large stress but rather approaches zero. Also, the shape of the curve does not agree well for small stresses near zero, because the derivative of the tangent modulus

$$\frac{\partial E_{tan}}{\partial \sigma} = \frac{\partial}{\partial \sigma} \left(\frac{\partial \sigma}{\partial \epsilon} \right) \text{ is equal to infinity rather than zero for } \sigma = 0 \text{ and}$$

$1 < n < 2$. For laminates not loaded in the direction of 0° fibers, the shape of the tangent modulus curve given by the Ramberg-Osgood equation agrees well with the data, because the secondary modulus of the material is zero and $n > 2$.

For laminate orientations containing 0° fibers, Poisson's ratio increases with stress for longitudinal tests and decreases with stress for transverse tests. For the $[\pm 45]_{2S}$ laminate (fig. 14), Poisson's ratio increases dramatically with stress and approaches unity.

In order to determine the strains at the onset of the nonlinearity, the tangent moduli are plotted against strain in figure 15 for strains up to 0.0012. The plots show that the laminates yielded at a strain of about 0.00025 except for the $[0]_{6T}$ laminates tested longitudinally. That laminate yielded at some-

what higher strains of about 0.0004, probably because the fibers are all in the loading direction and therefore cause virtually no concentration of strain in the matrix near the fibers. This yield strain is about equal to the yield strain of 0.0005 expected for the matrix itself.

Ultimate tensile strengths.— Figure 16 shows a comparison between experimental and predicted tensile strengths for the various boron/aluminum laminates. In the figure, ultimate tensile strengths are plotted against the percentages of 45° plies in the laminates. The symbols are plotted at the average of the experimental results and the tick marks indicate the extremes. The difference between the strengths of $[\pm 45/0_2]_S$ and $[0_2/\pm 45]_S$ specimens indicates a small effect of stacking sequence on strength.

The theoretical lines (both solid and dashed) were derived by assuming that in both longitudinal and transverse tests, the 0° plies fail first because

their failure strain is much smaller than that for the 45° plies. When failure of the 0° plies overloads the 45° plies, the laminate failure stresses are given by the solid lines in figure 16. For laminates with high percentages of 45° plies, however, the 45° plies are not overloaded and the laminates fail at strains and stresses higher than those at which the 0° plies fail; these failure stresses are shown by the dashed lines.

The equations for the lines were derived as follows. Assuming equal ply thicknesses, laminate theory gives the laminate stress in terms of the ply stresses as

$$\sigma = (\sigma)_{00} - [(\sigma)_{00} - (\sigma)_{450}] \frac{\Gamma}{100} \quad (12)$$

where Γ is the percentage of 45° plies and $(\sigma)_{00}$ and $(\sigma)_{450}$ are the stresses in the 0° and 45° plies, respectively. Thus, the laminate stress when the 0° plies fail is

$$F_{tu} = (F_{tu})_{00} - [(F_{tu})_{00} - (\sigma_{\epsilon})_{450}] \frac{\Gamma}{100} \quad (13)$$

where $(F_{tu})_{00}$ is the ultimate tensile strength of the 0° plies and $(\sigma_{\epsilon})_{450}$ is the stress in the 45° plies at the strain corresponding to failure of the 0° plies. Similarly, with the 0° plies having failed first, the laminate stress when the 45° plies fail is given by equation (12) with $(\sigma)_{00} = 0$ and $(\sigma)_{450} = (F_{tu})_{450}$, where $(F_{tu})_{450}$ is the ultimate tensile strength of the 45° plies. Thus,

$$F_{tu} = (F_{tu})_{450} \frac{\Gamma}{100} \quad (14)$$

The strength of the laminates, therefore, is given by the larger of the values calculated from equations (13) and (14). The values of F_{tu} and σ_{ϵ} given in the following table were used to calculate the lines in figure 16. The solid and dashed lines are given by equations (13) and (14), respectively. Average properties of the $[0]_{6T}$ and $[\pm 45]_{2S}$ laminates in tables I and V were

used for the 0° and 45° ply properties, respectively, and σ_{ϵ} for the 45° plies was determined from the average Ramberg-Osgood equations for the $[\pm 45]_{2S}$

laminates. The agreement between the predicted and experimental results in figure 16 is good.

	$(F_{tu})_{00}$, MPa	$(\epsilon_{tu})_{00}$	$(\sigma_{\epsilon})_{450}$, MPa	$(F_{tu})_{450}$, MPa
Longitudinal	1672	0.007908	144.8	220.6
Transverse	115.3	.002084	98.6	195.8

Elastic constants.— Average elastic constants were calculated for the initial linear portions of the stress-strain curves using lamina properties and laminate theory, and were then compared with the measured values. The average measured elastic constants for the $[0]_{6T}$ laminate were used for the lamina con-

stants in the analysis. The lamina shear modulus G_{12} , which was not measured, was calculated by

$$G_{12} = \frac{E_y}{2(1 + \nu_{yx})} \quad (15)$$

where E_y and ν_{yx} are the constants for the $[\pm 45]_{2S}$ laminate orientation.

Equation (15) was derived from equation (1) of reference 7. Substituting the average values from table V into equation (15) and averaging the G_{12} for the longitudinal and transverse tests gives $G_{12} = 48.68$ GPa. All the calculated elastic constants are listed in table VI.

Figure 17 shows the calculated constants and the measured elastic constants plotted against the percentage of 45° plies for both the longitudinal and transverse tests. The average and extreme values of the measured constants are shown. The measured values for the $[\pm 45/0_2]_S$ and $[0_2/\pm 45]_S$ laminates show

only a small effect of stacking sequence. The values calculated by laminate theory are higher than the average measured values by as much as 10 percent for Young's modulus and by as much as 20 percent for Poisson's ratio. The correlation cannot be improved by changing the value of lamina shear modulus because Young's modulus for the laminates increases with G_{12} and Poisson's ratio decreases with G_{12} .

The ratios of the products $\nu_{xy}E_y$ and $\nu_{yx}E_x$ were calculated from the average measured elastic constants and the results are shown in the following table. As anticipated for the orthotropic laminates, the ratios of the products were approximately equal to 1.

Laminate orientation	$\nu_{yx}E_x/\nu_{xy}E_y$
$[0]_{6T}$	1.011
$[0_2/\pm 45]_S$.986
$[\pm 45/0_2]_S$	1.001
$[0/\pm 45]_S$.986
$[\pm 45]_{2S}$	1.024

Note that the linear region of the stress-strain curves, for which the elastic constants were calculated, does not characterize the laminates over a significant part of their working range.

Cyclic Tensile Tests

Three loading cycles did not affect the stress and strain at failure for any of the boron/aluminum laminates. The ultimate tensile stress and strain for each cyclic test are presented in table VII, and these values are within the extremes for the static tests given in tables I to V. However, the laminates exhibited permanent strain on unloading. The permanent strains, which increased with applied stress and with the proportion of 45° plies, were significant - especially for the $[\pm 45]_{2S}$ laminate. Figures 18 to 22 show the

stress-strain curves for three cycles of loading for one longitudinal and one transverse test of each laminate orientation.

The composite, with the matrix in the "as fabricated" condition, strain-hardened like metals, and the average Ramberg-Osgood curves for monotonic loading form upper envelopes for the cyclic curves. The yield strengths increased dramatically with each load cycle. The hysteresis loops were much more pronounced when some fibers were in the loading direction, probably because the fibers caused the aluminum to yield in compression when unloading from the higher strains. The residual strains were higher for laminates with more 45° plies and were an order of magnitude higher for the $[\pm 45]_{2S}$ laminate than for laminates with 0° plies.

SUMMARY OF RESULTS

The tensile behavior of five types of boron/aluminum laminates ($[0]_{6T}$, $[\pm 45]_{2S}$, $[0/\pm 45]_S$, $[0_2/\pm 45]_S$, and $[\pm 45/0_2]_S$) was investigated. Longitudinal and transverse stress-strain curves were obtained for monotonic loading to failure and for three cycles of loading to successively higher load levels. The Ramberg-Osgood equation was fitted to the stress-strain data to obtain average curves for the various laminate orientations. The following were concluded from the study:

1. For the laminates with 0° plies in the loading direction, the ultimate strengths varied linearly with the percentage of 0° plies in the composite. The strengths predicted by assuming that the 0° plies failed first correlated well with the experimental results.
2. The stress-strain curves for all the laminates were nonlinear except at strains below about 0.00025. In the linear region, measured Young's modulus and Poisson's ratio were within 10 to 20 percent, respectively, of those calculated from laminate theory. However, the linear region does not characterize the laminates over a significant part of their working range.
3. The nonlinearity in the stress-strain curves was greater for higher percentages of 45° plies in the laminate.
4. Laminates without fibers in the loading direction exhibited a very large scatter in the stress and strain at failure.

5. Three cycles of loading did not affect the ultimate stress and strain of the boron/aluminum laminates. The laminates, however, exhibited a permanent strain on unloading. As with the nonlinearity in the stress-strain curves, the amount of permanent strain was greater for laminates with more 45° plies.

6. The Ramberg-Osgood equation fitted the experimental stress-strain curves well.

Langley Research Center
National Aeronautics and Space Administration
Hampton, VA 23665
December 12, 1977

APPENDIX

METHOD FOR FITTING RAMBERG-OSGOOD EQUATION TO STRESS-STRAIN DATA

Equations (7) were fitted to the stress-strain data for longitudinal specimens and equations (8) to the data for transverse specimens. These equations are repeated here for convenience.

$$\left. \begin{aligned} \epsilon_y &= \frac{\sigma_y}{E_y} + (b_{yy}\sigma_y)^{n_{yy}} \\ \epsilon_x &= -\frac{\sigma_y \nu_{yx}}{E_y} - (b_{yx}\sigma_y)^{n_{yx}} \end{aligned} \right\} \quad (A1)$$

$$\left. \begin{aligned} \epsilon_y &= -\frac{\sigma_x \nu_{xy}}{E_x} - (b_{xy}\sigma_x)^{n_{xy}} \\ \epsilon_x &= \frac{\sigma_x}{E_x} + (b_{xx}\sigma_x)^{n_{xx}} \end{aligned} \right\} \quad (A2)$$

Data from each test were fitted separately using a least-squares method, and the resulting constants were used to define an average curve for each laminate. An iterative least-squares procedure to determine E (or E/ν), b , and n simultaneously would not converge satisfactorily. Thus, the following two-step iterative procedure was used where b and n were determined simultaneously and E (or E/ν) separately.

First, the values of E and E/ν were determined for each test by fitting the linear terms on the right side of equations (A1) and (A2) to only the data in the initial linear region. (Strains in the direction of load in the linear region were less than 0.00025.) A conventional least-squares method was used. Poisson's ratio was then determined from the ratio of E and E/ν .

Next, using the calculated values of E and ν , the constants b and n were determined by fitting equations (A1) and (A2) to all the data from each test. The following iterative, least-squares method (ref. 8, pp. 336-337) was used. The Ramberg-Osgood equation (eq. (6) in the main text),

$$\epsilon = \frac{\sigma}{E} + (b\sigma)^n \quad (A3)$$

was expanded into a Taylor's series in terms of b and n , and the higher order terms were dropped. Thus,

APPENDIX

$$\epsilon = \epsilon(b_0, n_0) + \delta b \frac{\partial \epsilon(b_0, n_0)}{\partial b} + \delta n \frac{\partial \epsilon(b_0, n_0)}{\partial n} \quad (A4)$$

where

$$\left. \begin{aligned} b &= b_0 + \delta b \\ n &= n_0 + \delta n \end{aligned} \right\} \quad (A5)$$

The b_0 and n_0 were taken as approximations to b and n and δb and δn as corrections to b_0 and n_0 . By substituting equation (A3) for $\epsilon(b, n)$, equation (A4) becomes

$$\epsilon = \frac{\sigma}{E} + (b_0 \sigma)^{n_0} + n_0 \sigma (b_0 \sigma)^{n_0-1} \delta b + (b_0 \sigma)^{n_0} (\ln b_0 \sigma) \delta n \quad (A6)$$

The corrections δb and δn were calculated to minimize the sum of the squares of the residuals. The residual was the measured strain less the strain calculated by equation (A6).

The approximate values b_0 and n_0 were determined initially by passing equation (A3) through two of the data points: one corresponding to the ultimate strain, and the other to one-half of the ultimate strain. The new values of b and n calculated by equation (A5) were then used for approximate values to calculate new corrections. This procedure was repeated, generally less than 10 times, until the corrections were less than 1 percent of the values of b and n . Figure 23 shows examples of experimental stress-strain curves and the fitted Ramberg-Osgood curves. The agreement between these data and equations (A1) and (A2) is typical of all the data.

Figure 24 shows the calculated values of b and n plotted as $\ln b$ against n^{-1} for the longitudinal tests of the $[0_2/\pm 45]_S$ laminate orientation.

The lines show significant linear correlation between $\ln b$ and n^{-1} . All of the other data showed a similar linear correlation. An average Ramberg-Osgood equation for each laminate was defined by using the b and n values corresponding to the average values of $\ln b$ and n^{-1} . Thus, an average behavior was written

$$\epsilon = \frac{\sigma}{E} + \left(\sigma e^{\overline{\ln b}} \right) \left(\overline{n^{-1}} \right)^{-1} \quad (A7a)$$

$$\epsilon = \frac{\sigma \bar{v}}{E} + \left(\sigma e^{\overline{\ln b}} \right) \left(\overline{n^{-1}} \right)^{-1} \quad (A7b)$$

where \bar{E} , \bar{v} , $\overline{\ln b}$, and $\overline{n^{-1}}$ are the means of E , v , $\ln b$, and n^{-1} .

APPENDIX

Tables I to V contain the values of E , ν , $\ln b$, and n^{-1} for each test and the mean values for each laminate. For the $[0]_{6T}$ laminate tested trans-

versely, ϵ_y was virtually linear with stress σ_x . For these tests, the iterative procedure did not converge in 20 iterations. Therefore, values of $\ln b_{xy}$ and $(n_{xy})^{-1}$ are not given for these tests in table I. However, the corrections to b and n always made b^n successively smaller. Thus, the average value of $\ln b_{xy}$ is given as $-\infty$ so that the right-most term in equation (A7b) is zero.

REFERENCES

1. Elliott, S. Y.: Boron-Aluminum Skins for the DC-10 Aft Pylon - Final Report. NASA CR-132645, 1975.
2. Waszczak, J. P.: On the Applicability of Linear Elastic Fracture Mechanics to 5.6-Mil Boron/6061 Aluminum. AIAA Paper No. 75-786, May 1975.
3. Swanson, G. D.; and Hancock, J. R.: Off-Axis and Transverse Tensile Properties of Boron Reinforced Aluminum Alloys. Composite Materials: Testing and Design (Second Conference), ASTM STP 497, 1972, pp. 469-482.
4. Advanced Composites Design Guide. Volume I - Design. Third Edition (Second Revision). Contract No. F33615-74-C-5075, Flight Dyn. Lab., U.S. Air Force, Sept. 1976.
5. Ashton, J. E.; Halpin, J. C.; and Petit, P. H.: Primer on Composite Materials: Analysis. Technomic Pub. Co., Inc., c.1969.
6. Ramberg, Walter; and Osgood, William R.: Description of Stress-Strain Curves by Three Parameters. NACA TN 902, 1943.
7. Rosen, B. Walter: A Simple Procedure for Experimental Determination of the Longitudinal Shear Modulus of Unidirectional Composites. J. Compos. Mater., vol. 6, Oct. 1972, pp. 552-554.
8. Guest, P. G.: Numerical Methods of Curve Fitting. Cambridge Univ. Press, 1961.

TABLE I.- STRESS-STRAIN PARAMETERS FOR $[0]_{6T}$ LAMINATE

(a) Longitudinal tests

Specimen number	F_{tu} , MPa	ϵ_{tu}	E_y , GPa	ν_{yx}	$\ln b_{yy}$	$(n_{yy})^{-1}$	$\ln b_{yx}$	$(n_{yx})^{-1}$
0128	1790	0.008477	^a 237.3	^a 0.2049	-25.51	0.6168	-26.44	0.7088
0228	1794	.008246	240.2	.2093	-24.02	.4897	-25.34	.4709
0328	1644	.007875	238.8	.2016	-26.12	.7203	-26.85	.7713
0428	1726	.007889	235.0	.1948	-26.12	.7018	-27.60	.8681
0528	1737	.008378	241.9	.2186	-25.97	.6977	-26.56	.7127
0628	1342	.006581	230.5	.2000	-26.23	.7434	-26.88	.7901
Average	1672	0.007908	237.3	0.2049	-25.66	0.6616	-26.61	0.7203

(b) Transverse tests

Specimen number	F_{tu} , MPa	ϵ_{tu}	E_x , GPa	ν_{xy}	$\ln b_{xx}$	$(n_{xx})^{-1}$	$\ln b_{xy}$ (b)	$(n_{xy})^{-1}$ (b)
0129	106.5	0.001173	139.2	0.1027	-19.72	0.1641	-----	-----
0329	87.29	.000819	135.6	.1161	-20.14	.2232	-----	-----
0429	111.6	.001897	137.0	.1108	-19.55	.1529	-----	-----
0529	118.7	.001560	139.0	.1227	-19.57	.1366	-----	-----
0629	118.9	.003017	145.4	.1375	-19.82	.1997	-----	-----
0929	99.49	.001251	154.9	.1172	-19.63	.1667	-----	-----
1029	164.8	.004872	150.5	.1384	-19.98	.1913	-----	-----
Average	115.3	0.002084	143.1	0.1208	-19.77	0.1764	∞	1.0

^aElastic constants could not be determined from data because ϵ_y was not measured below 0.00025. Thus, average elastic constants were assumed.

^bIterative calculation did not converge in 20 iterations; variation of ϵ_y with σ_x was virtually linear.

TABLE II.- STRESS-STRAIN PARAMETERS FOR $[0_2/+45]_S$ LAMINATE

(a) Longitudinal tests

Specimen number	F_{tu} , MPa	ϵ_{tu}	E_y , GPa	ν_{yx}	$\ln b_{yy}$	$(n_{yy})^{-1}$	$\ln b_{yx}$	$(n_{yx})^{-1}$
4128	792.8	0.007125	169.1	0.2757	-24.25	0.6346	-24.16	0.5543
4228	744.1	.006673	177.9	.2686	-24.21	.6312	-24.07	.5413
4328	753.5	.006831	175.9	.2594	-24.23	.6366	-24.34	.5809
4428	805.3	.007377	179.5	.2292	-24.42	.6736	-24.52	.6158
4528	808.4	.007452	179.4	.2535	-24.30	.6554	-24.38	.5893
4628	877.5	.007945	178.1	.2552	-24.37	.6547	-24.57	.6027
4928	841.4	.007504	179.5	.2617	-24.33	.6496	-24.38	.5879
5028	799.0	.007082	176.7	.2503	-24.28	.6391	-24.02	.5352
5128	781.7	.007048	176.4	.2526	-24.41	.6691	-24.24	.5759
5228	805.3	.007567	172.5	.2244	-24.30	.6558	-24.86	.6656
5328	792.3	.007337	172.7	.2337	-24.25	.6477	-24.83	.6581
Average	800.1	0.007267	176.2	0.2513	-24.30	0.6498	-24.40	0.5915

(b) Transverse tests

Specimen number	F_{tu} , MPa	ϵ_{tu}	E_x , GPa	ν_{xy}	$\ln b_{xx}$	$(n_{xx})^{-1}$	$\ln b_{xy}$	$(n_{xy})^{-1}$
4229	103.6	0.002026	128.9	0.1905	-20.51	0.3100	-21.92	0.3325
4329	103.6	.002081	131.1	.1891	-20.16	.2583	-22.21	.4998
4429	105.1	.002249	130.7	.1942	-20.50	.3143	-22.41	.4803
4529	106.7	.002230	130.8	.1885	-20.57	.3237	-21.97	.3873
4629	95.70	.002172	129.0	.2085	-20.35	.3062	-22.25	.2179
4929	97.28	.002725	123.0	.1692	-20.23	.2947	-25.74	.8361
5029	89.42	.001563	126.4	.1906	-19.91	.2304	-22.49	.2067
5129	116.1	.002788	130.7	.2057	-20.42	.2981	-22.59	.2244
5229	139.7	.005884	134.4	.1907	-19.95	.2165	-21.00	.2849
5329	135.0	.004515	136.2	.2043	-20.10	.2430	-21.99	.2434
Average	109.2	0.002823	130.1	0.1931	-20.27	0.2795	-22.46	0.3713

TABLE III.- STRESS-STRAIN PARAMETERS FOR $[\pm 45/0_2]_S$ LAMINATE

(a) Longitudinal tests

Specimen number	F_{tu} , MPa	ϵ_{tu}	E_y , GPa	ν_{yx}	$\ln b_{yy}$	$(n_{yy})^{-1}$	$\ln b_{yx}$	$(n_{yx})^{-1}$
5628	926.4	0.008279	181.3	0.2394	-24.50	0.6739	-25.24	0.7106
5728	901.6	.008224	178.8	.2846	-24.38	.6581	-24.83	.6434
5828	906.2	.008075	175.7	.2274	-24.55	.6781	-25.16	.7009
5928	907.8	.008242	174.2	.2560	-24.36	.6500	-25.06	.6882
Average	910.5	0.008205	177.5	0.2519	-24.45	0.6650	-25.07	0.6858

(b) Transverse tests

Specimen number	F_{tu} , MPa	ϵ_{tu}	E_x , GPa	ν_{xy}	$\ln b_{xx}$	$(n_{xx})^{-1}$	$\ln b_{xy}$	$(n_{xy})^{-1}$
5729	102.0	0.002269	134.3	0.2036	-20.80	0.3682	-21.24	0.3289
5829	154.6	.008785	130.7	.1842	-20.02	.2386	-21.22	.3182
5929	112.9	.003055	129.5	.1735	-20.64	.3403	-20.96	.2986
5629	118.6	.012040	144.3	.2074	-20.49	.3142	-31.35	1.751
Average	139.5	0.006537	134.7	0.1922	-20.49	0.3153	-23.69	0.6742

TABLE IV.- STRESS-STRAIN PARAMETERS FOR $[0/\pm 45]_S$ LAMINATE

(a) Longitudinal tests

Specimen number	F_{tu} , MPa	ϵ_{tu}	E_y , GPa	ν_{yx}	$\ln b_{yy}$	$(n_{yy})^{-1}$	$\ln b_{yx}$	$(n_{yx})^{-1}$
2628	606.1	0.007138	165.9	0.2735	-23.55	0.5932	-23.39	0.5084
2728	591.4	.006988	164.6	.2804	-23.61	.6065	-23.28	.5055
2828	597.7	.007285	158.4	.2950	-23.46	.5837	-23.15	.4718
2928	553.5	.006448	161.3	.3027	-23.31	.5581	-23.29	.4828
3028	591.4	.007407	162.2	.2895	-23.45	.5863	-23.07	.4696
3128	639.8	.007615	157.5	.3112	-23.40	.5619	-23.30	.4573
3428	635.6	.007856	155.7	.2948	-23.25	.5388	-23.41	.4684
3528	513.5	.005608	150.6	.3163	-23.09	.5081	-22.65	.3703
3628	576.6	.007252	163.1	.3008	-23.55	.6084	-23.33	.4994
3728	559.8	.006964	155.7	.2760	-23.43	.5814	-23.20	.4863
3828	530.3	.006535	156.0	.2620	-23.39	.5834	-23.50	.5330
Average	581.4	0.007008	159.2	0.2911	-23.41	0.5736	-23.23	0.4775

(b) Transverse tests

Specimen number	F_{tu} , MPa	ϵ_{tu}	E_x , GPa	ν_{xy}	$\ln b_{xx}$	$(n_{xx})^{-1}$	$\ln b_{xy}$	$(n_{xy})^{-1}$
2629	179.9	0.006231	136.3	0.2430	-20.31	0.2498	-20.77	0.2649
2729	169.0	.005429	136.8	.2245	-20.45	.2783	-21.36	.3387
2829	138.4	.005785	122.6	.2446	-19.94	.2170	-21.34	.3342
2929	184.8	.006269	135.4	.2548	-20.68	.3109	-21.18	.3078
3029	164.2	.005930	126.1	.2352	-20.41	.2830	-22.33	.4496
3129	119.9	.002361	125.0	.2398	-20.54	.2990	-22.20	.2152
3429	130.4	.002535	129.4	.2078	-20.35	.2583	-21.83	.3633
3529	143.1	.003366	131.5	.2492	-20.49	.2815	-20.32	.2063
3629	128.4	.004192	129.0	.2267	-20.03	.2270	-21.10	.3007
3729	117.8	.002364	134.2	.2172	-20.56	.3048	-22.65	.1877
3829	124.2	.002537	118.7	.2401	-19.93	.2014	-20.12	.1938
Average	145.5	0.004273	129.5	0.2348	-20.34	0.2646	-21.38	0.2875

TABLE V.- STRESS-STRAIN PARAMETERS FOR $[\pm 45]_{2S}$ LAMINATE

(a) Longitudinal tests

Specimen number	F_{tu} , MPa	ϵ_{tu} (a)	E_y , GPa	ν_{yx}	$\ln b_{yy}$	$(n_{yy})^{-1}$	$\ln b_{yx}$	$(n_{yx})^{-1}$
1128	194.6	0.02084	127.9	0.3212	-19.87	0.2245	-19.81	0.1951
1228	191.5	.02052	119.0	.3269	-19.77	.2206	-19.73	.1970
1328	220.6	.02525	134.0	.3216	-19.88	.2214	-19.82	.1948
1428	203.8	.02509	120.3	.3212	-19.77	.2153	-19.77	.1999
1528	164.7	.01506	125.7	.3039	-19.79	.2105	-19.77	.1882
1628	260.5	.02581	127.4	.3377	-20.01	.2147	-19.95	.1868
1928	221.4	.01998	128.3	.3212	-19.89	.2017	-19.83	.1719
2028	244.4	.02392	137.6	.3479	-19.91	.1949	-19.88	.1760
2128	183.1	.02030	129.1	.3302	-19.80	.2136	-19.80	.1967
2228	290.3	.02789	129.3	.3427	-19.84	.2195	-19.77	.1957
2428	255.9	.01719	129.5	.3150	-19.86	.2179	-19.82	.1965
2518	216.0	.03457	114.4	.3068	-19.89	.2082	-19.89	.1958
Average	220.6	0.02304	126.9	0.3247	-19.86	0.2136	-19.82	0.1912

(b) Transverse tests

Specimen number	F_{tu} , MPa	ϵ_{tu} (a)	E_x , GPa	ν_{xy}	$\ln b_{xx}$	$(n_{xx})^{-1}$	$\ln b_{xy}$	$(n_{xy})^{-1}$
1129	166.2	0.02019	120.1	0.3261	-19.67	0.1990	-19.62	0.1730
1229	173.9	.01529	131.2	.3074	-19.70	.1983	-19.66	.1737
1329	142.5	.008621	125.2	.3002	-19.81	.2173	-19.77	.1934
1429	186.9	.02620	119.8	.3182	-19.63	.1936	-19.59	.1710
1529	185.4	.02665	118.5	.3306	-19.71	.2088	-19.71	.1889
1629	195.3	.03074	128.0	.3440	-19.81	.2101	-19.76	.1839
1929	193.1	.01648	133.9	.3182	-19.91	.2068	-19.83	.1723
2029	215.3	.03189	^b 126.2	^b .3224	-19.81	.1956	-19.79	.1743
2129	244.4	.02502	129.3	.3408	-19.89	.2244	-19.83	.1985
2229	263.5	.01846	130.8	.3044	-19.92	.2302	-19.80	.1915
2429	187.7	.03077	125.3	.3342	-19.77	.2088	-19.68	.1747
Average	195.8	0.02276	126.2	0.3224	-19.78	0.2084	-19.73	0.1814

^aStrain at which gage failed.

^bElastic constants could not be determined from data because ϵ_y was not measured below 0.00025. Thus, the average elastic constants from the other tests were used to fit the Ramberg-Osgood equation.

TABLE VI.- ELASTIC CONSTANTS CALCULATED FROM LAMINATE THEORY

Laminate orientation	E_y , GPa	E_x , GPa	ν_{yx}	ν_{xy}	G_{xy} , GPa
$[0]_{6T}$	237.9	144.4	0.2040	0.1225	48.68
$[0_2/\pm 45]_S$	188.5	144.0	.3056	.2334	65.82
$[\pm 45/0_2]_S$	188.5	144.0	.3056	.2334	65.82
$[0/\pm 45]_S$	171.2	142.2	.3375	.2804	71.43
$[\pm 45]_{2S}$	136.2	136.2	.3986	.3986	82.94

TABLE VII.- ULTIMATE TENSILE STRENGTH AND STRAIN FOR CYCLIC TESTS

Laminate orientation	Specimen number	ϵ_{tu}	F_{tu} , MPa
Longitudinal tests			
$[0]_{6T}$	0928	0.007449	1646
$[0]_{6T}$	1028	.008269	1544
$[0_2/\pm 45]_S$	5428	.007020	763.9
$[0_2/\pm 45]_S$	5528	.006925	736.4
$[\pm 45/0_2]_S$	6028	.007942	871.5
$[0/\pm 45]_S$	3928	.006884	552.0
$[0/\pm 45]_S$	4028	.006955	550.7
$[\pm 45]_{2S}$	2328	a.024880	236.4
$[\pm 45]_{2S}$	2528	a.021010	242.2
Transverse tests			
$[0]_{6T}$	0319	0.000577	70.81
$[0]_{6T}$	0419	.000882	92.80
$[0_2/\pm 45]_S$	5429	.002406	110.2
$[0_2/\pm 45]_S$	5529	.005558	135.6
$[\pm 45/0_2]_S$	6029	.005251	135.6
$[0/\pm 45]_S$	3929	.001680	111.2
$[0/\pm 45]_S$	4029	.002639	124.5
$[\pm 45]_{2S}$	2329	a.016050	168.0
$[\pm 45]_{2S}$	2529	a.022260	216.1

^aStrain at which gage failed.

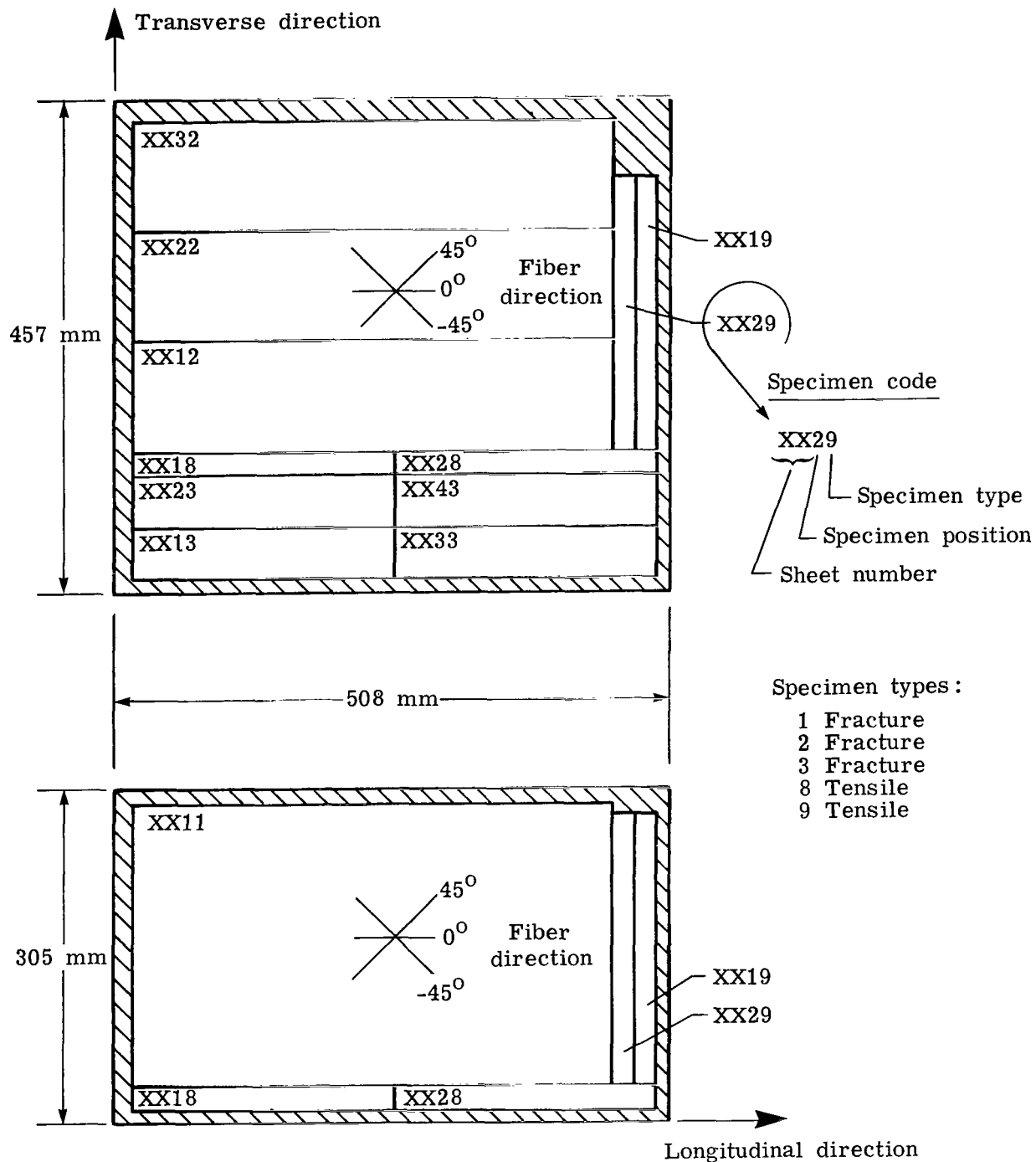
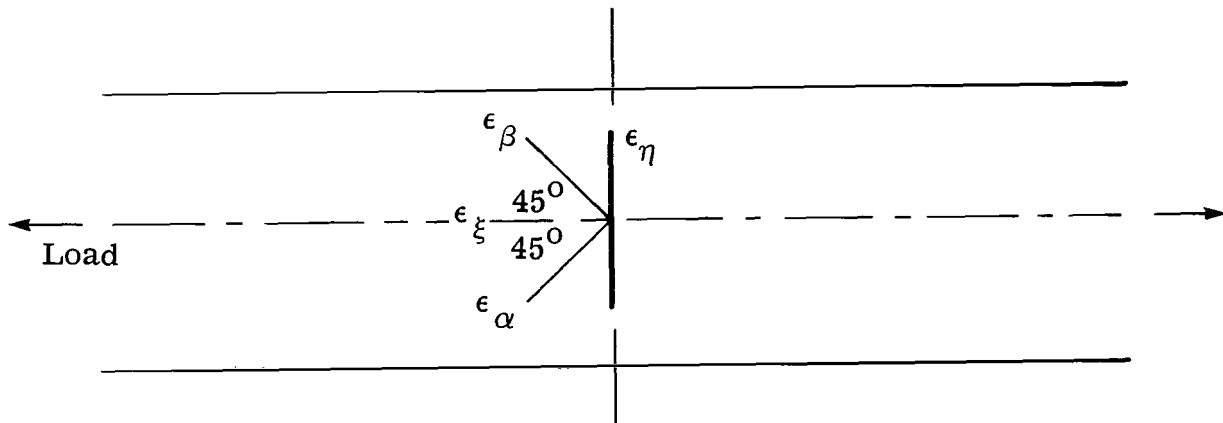


Figure 1.- Specimen layouts for the two sizes of boron/aluminum sheets.



Channel numbers	Signal
1	Strain gage voltage
2	Load
3	ϵ_α strain (front)
4	ϵ_α strain (back)
5	Load
6	ϵ_ξ strain (front)
7	ϵ_ξ strain (back)
8	Load
9	ϵ_β strain (front)
10	ϵ_β strain (back)
11	Load
12	Peak-load reader

Figure 2.- Recording format for data.

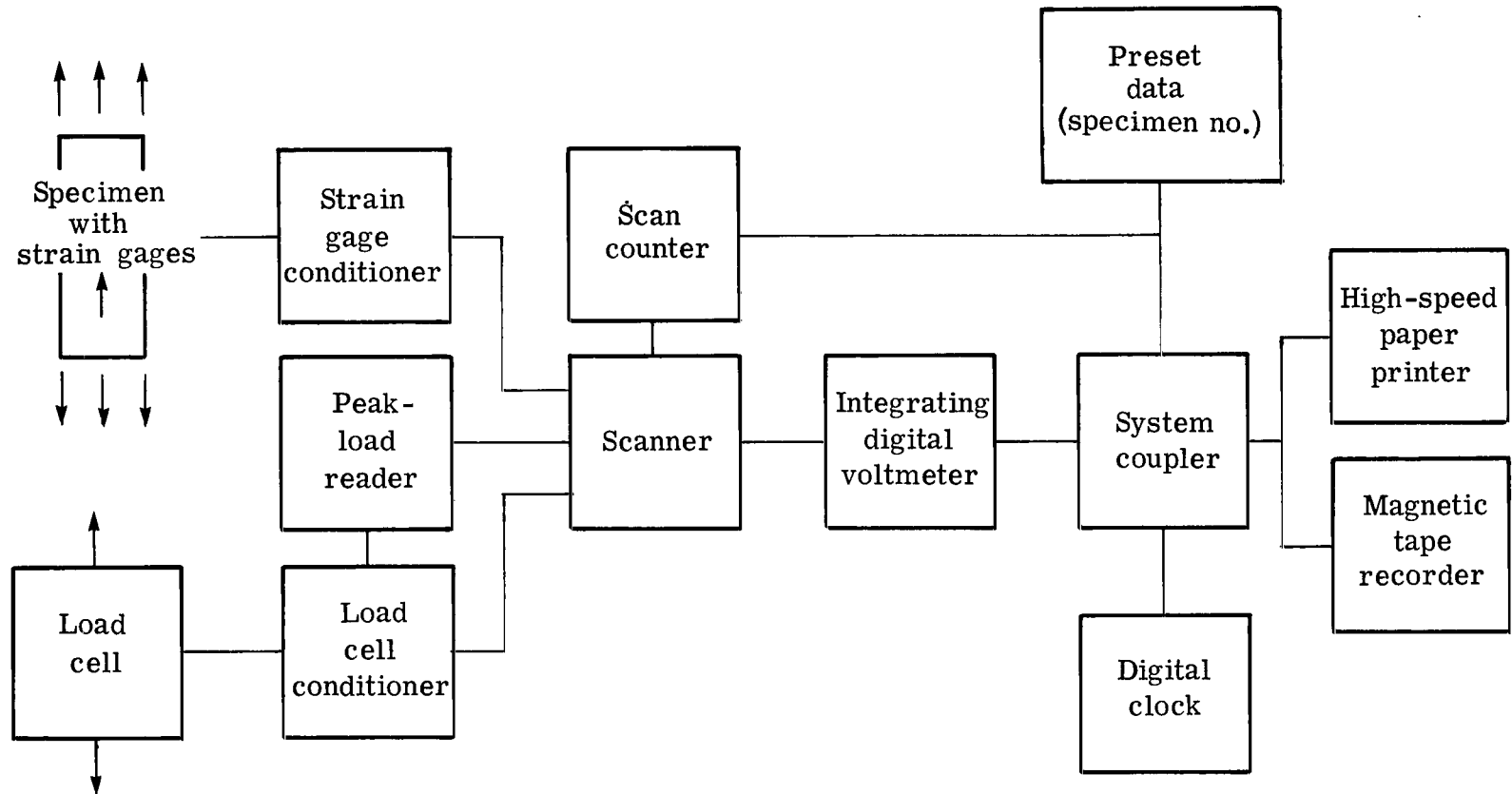
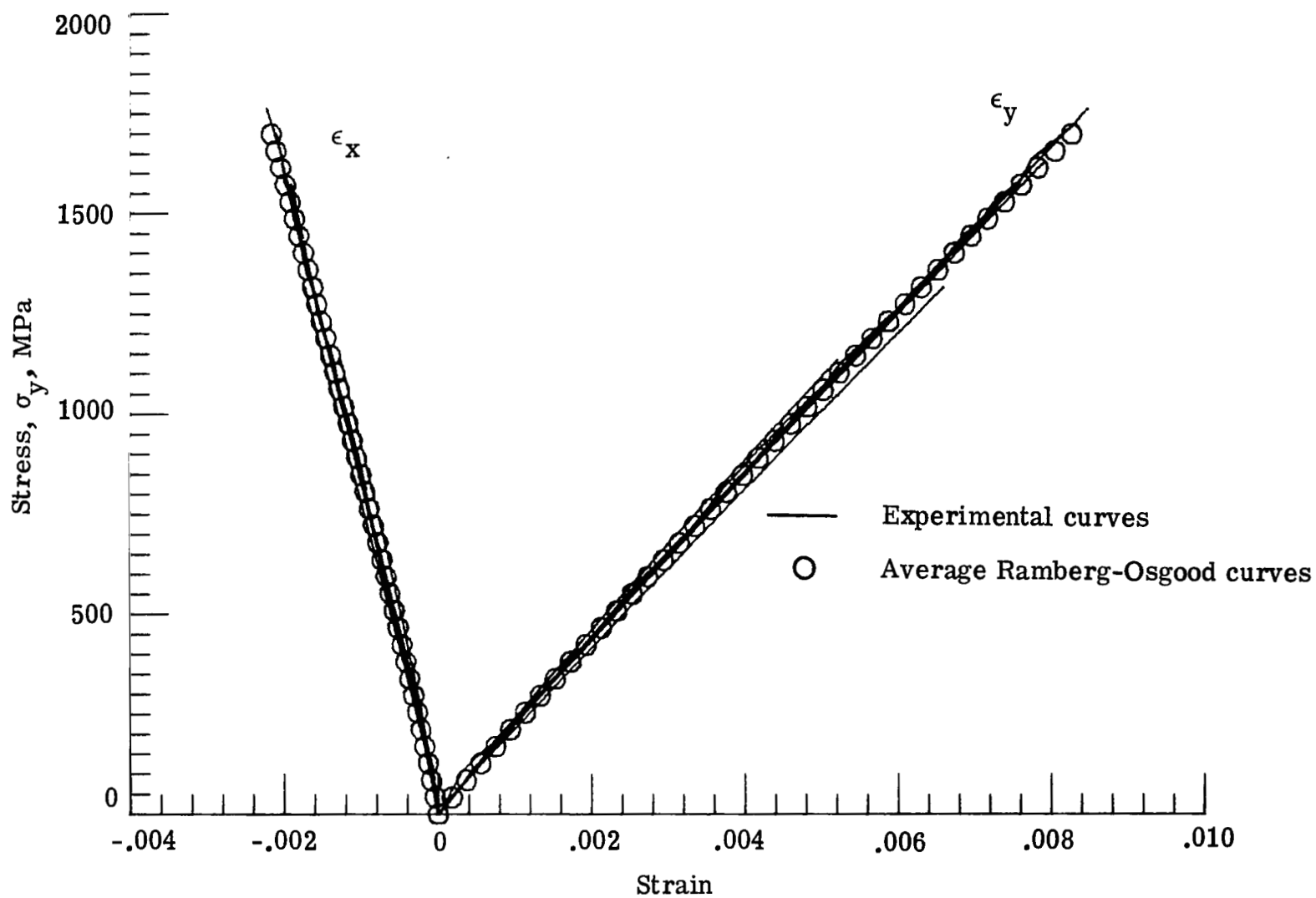
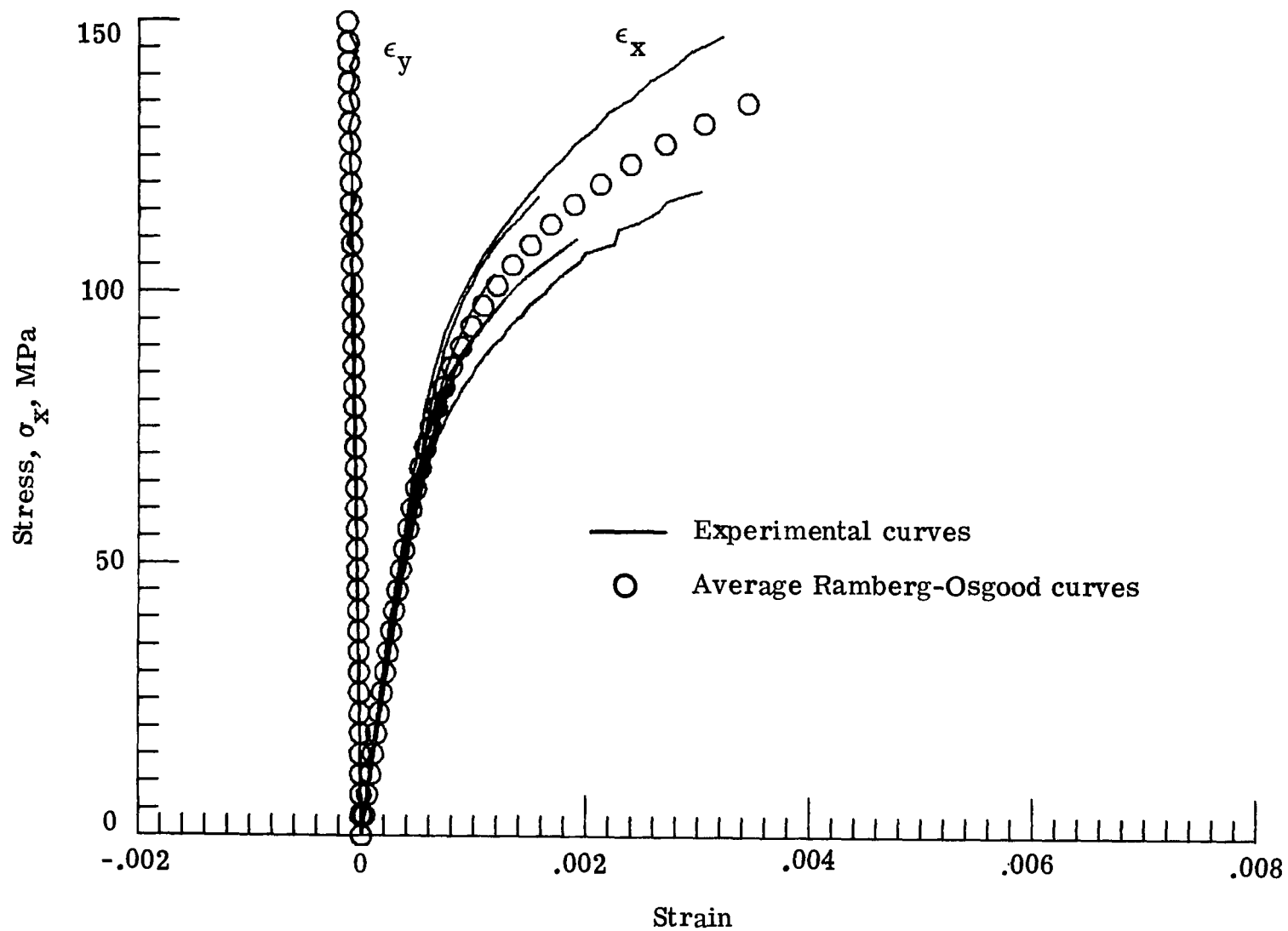


Figure 3.- Schematic diagram of data acquisition system.



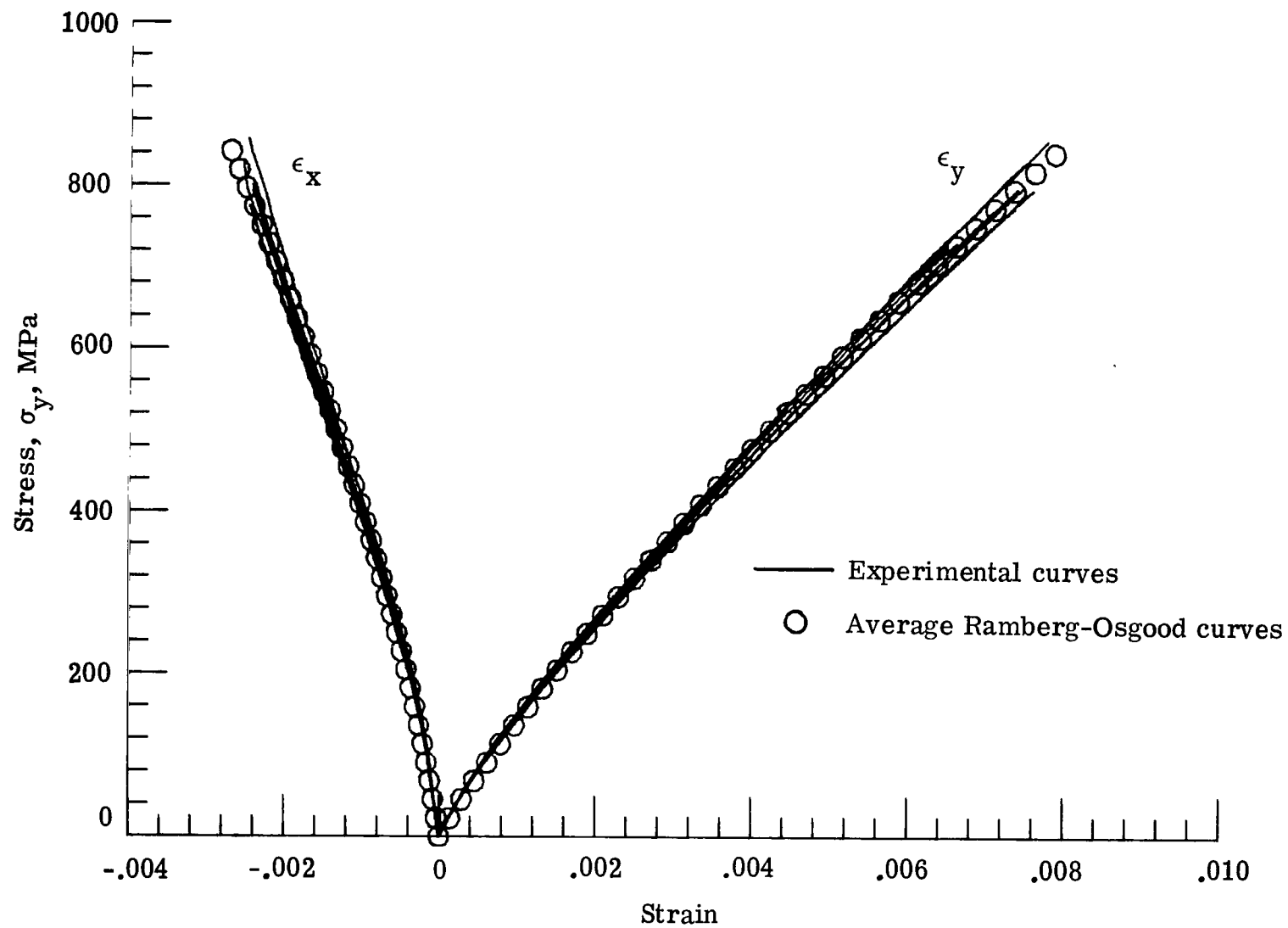
(a) Longitudinal tests.

Figure 4.- Stress-strain curves for $[0]_{6T}$ laminates.



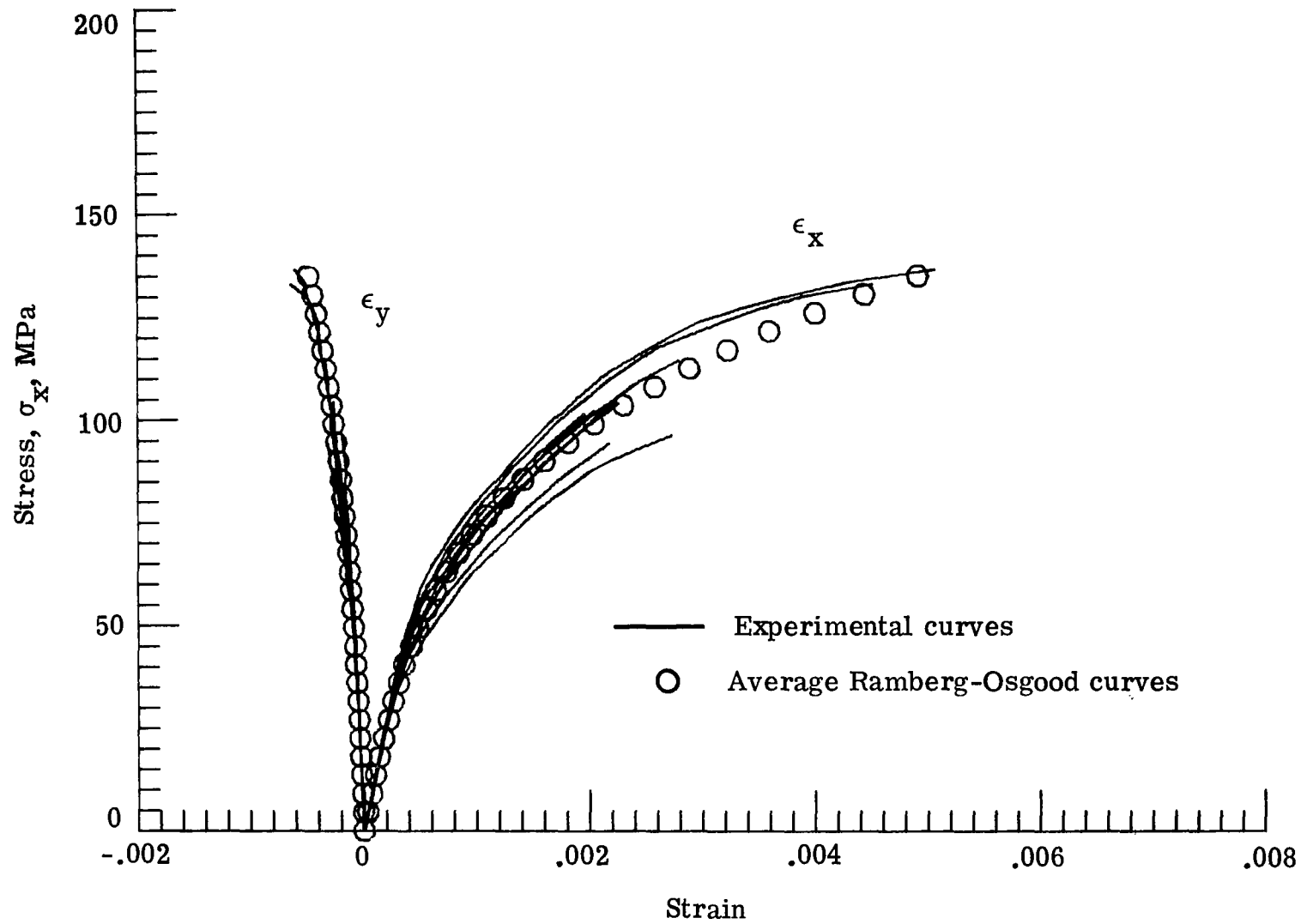
(b) Transverse tests.

Figure 4.- Concluded.



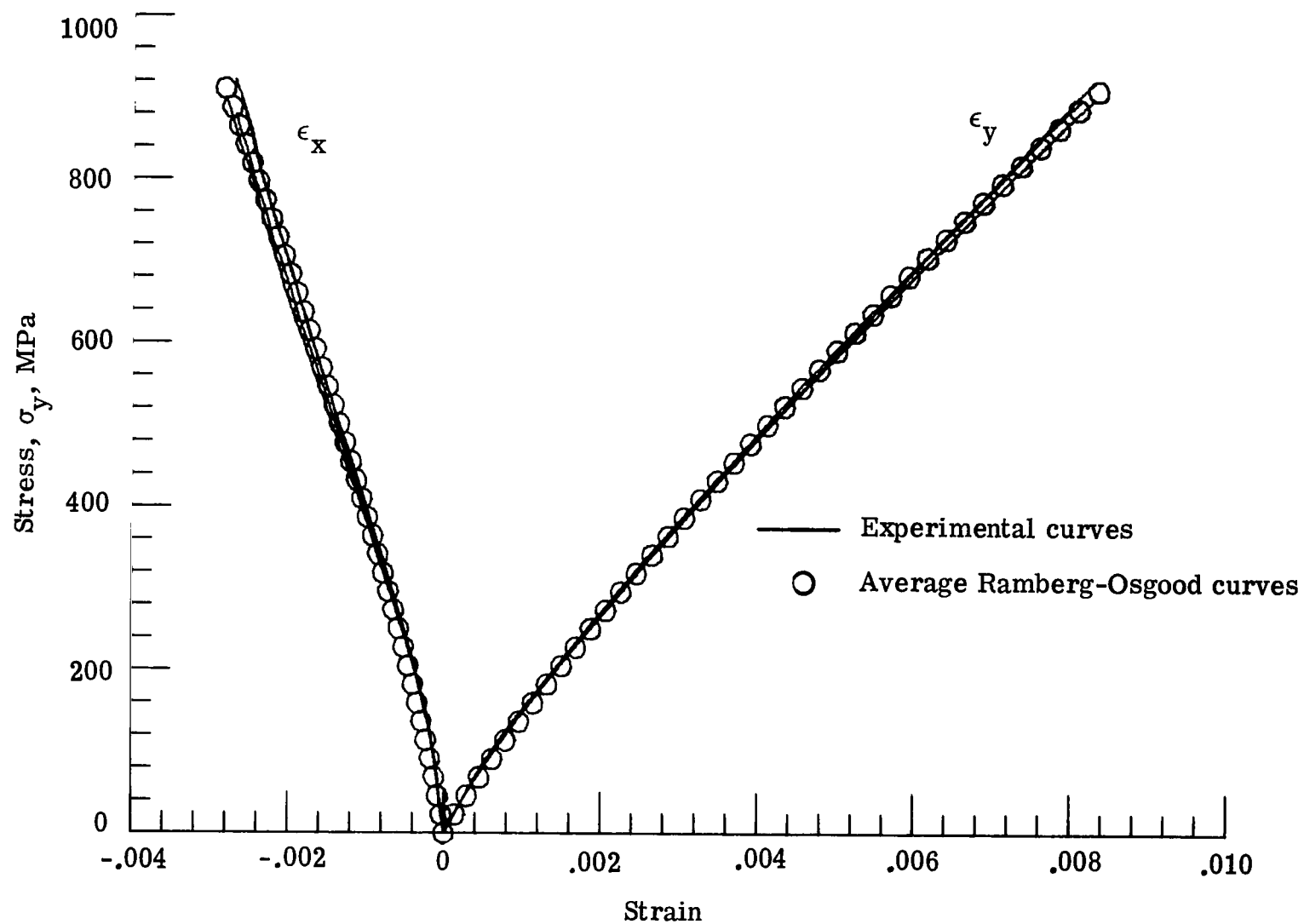
(a) Longitudinal tests.

Figure 5.- Stress-strain curves for $[0_2/+45]_S$ laminates.



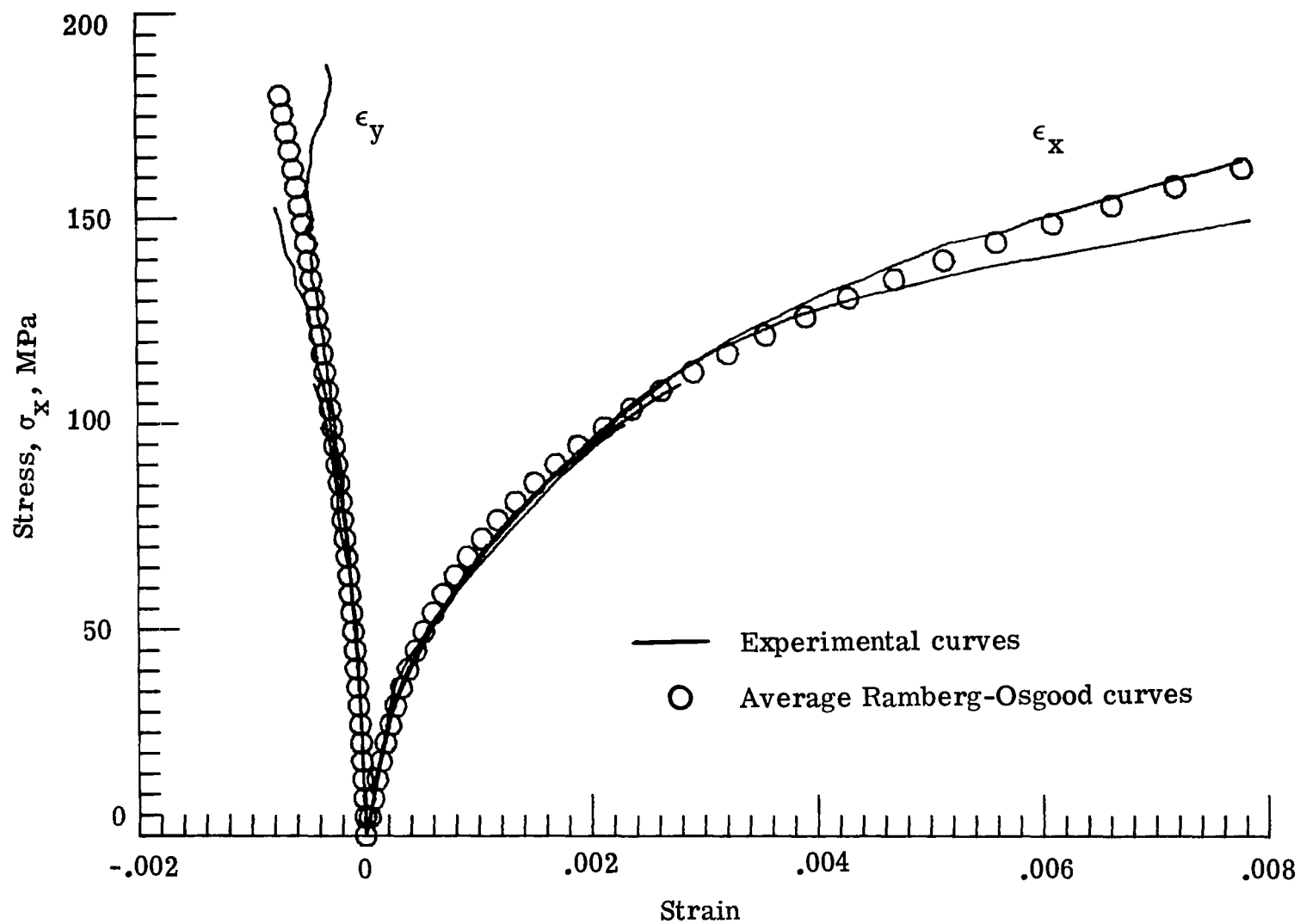
(b) Transverse tests.

Figure 5.- Concluded.



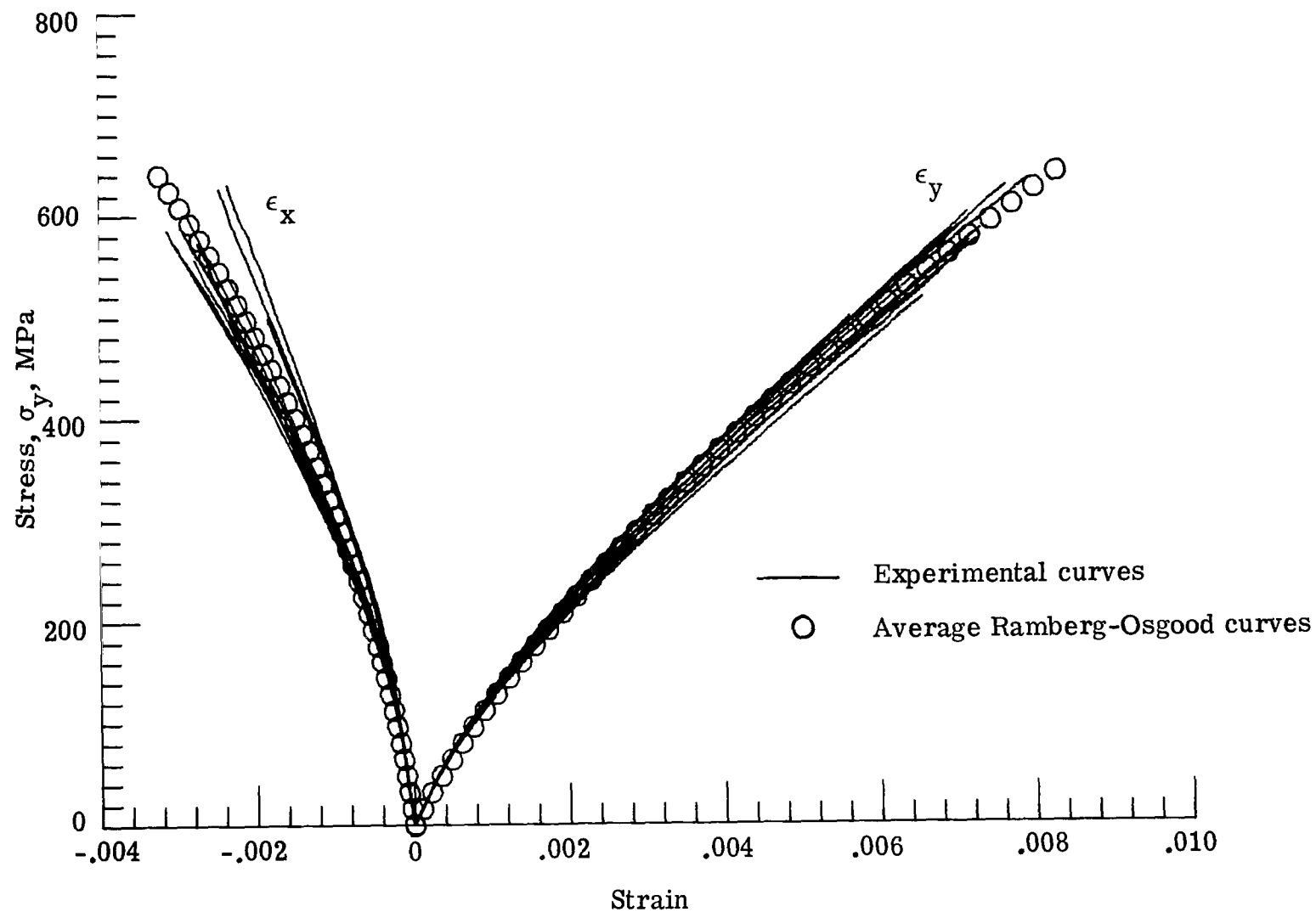
(a) Longitudinal tests.

Figure 6.- Stress-strain curves for $[\pm 45/0_2]_S$ laminates.



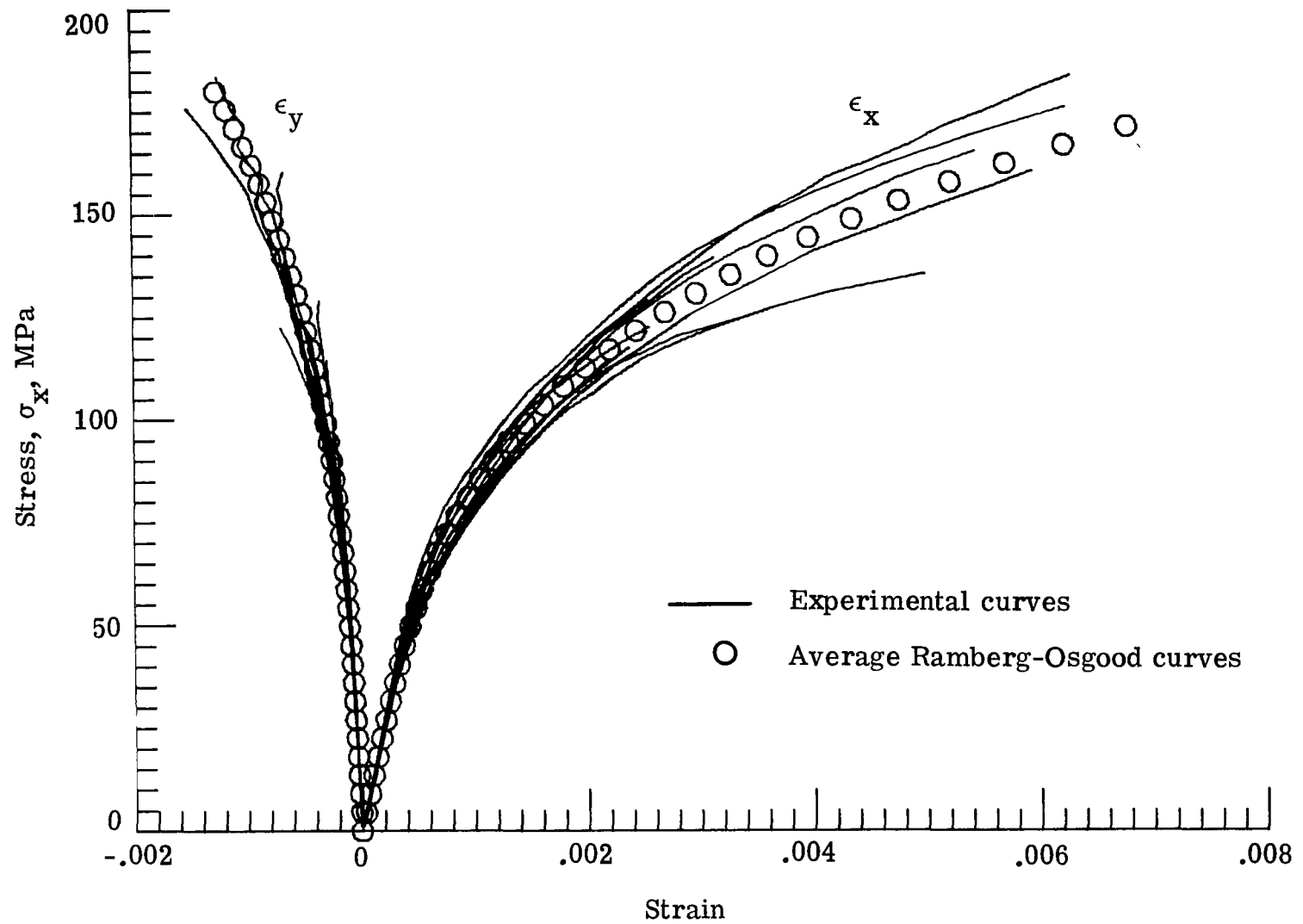
(b) Transverse tests.

Figure 6.- Concluded.



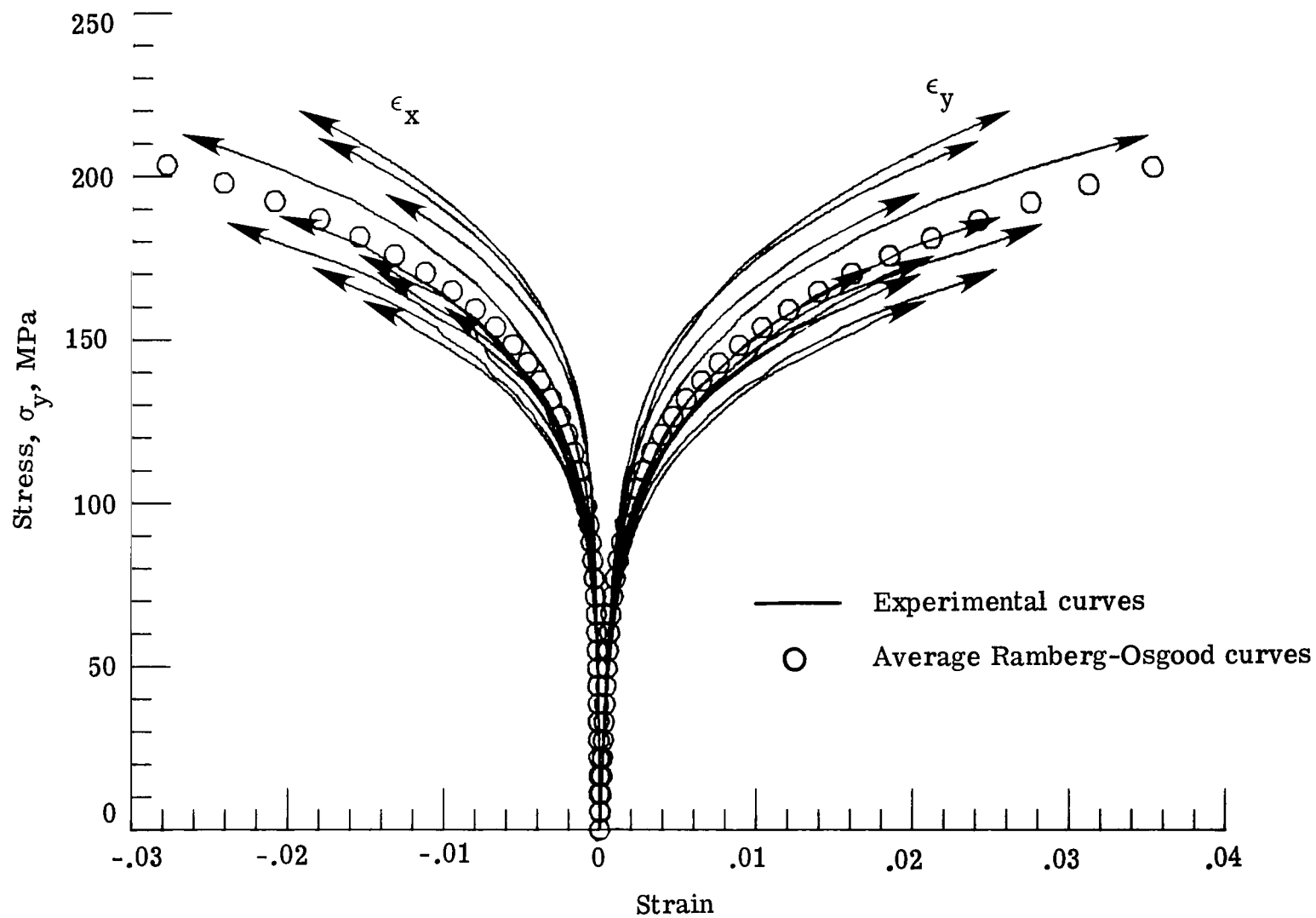
(a) Longitudinal tests.

Figure 7.- Stress-strain curves for $[0/\pm 45]_S$ laminates.



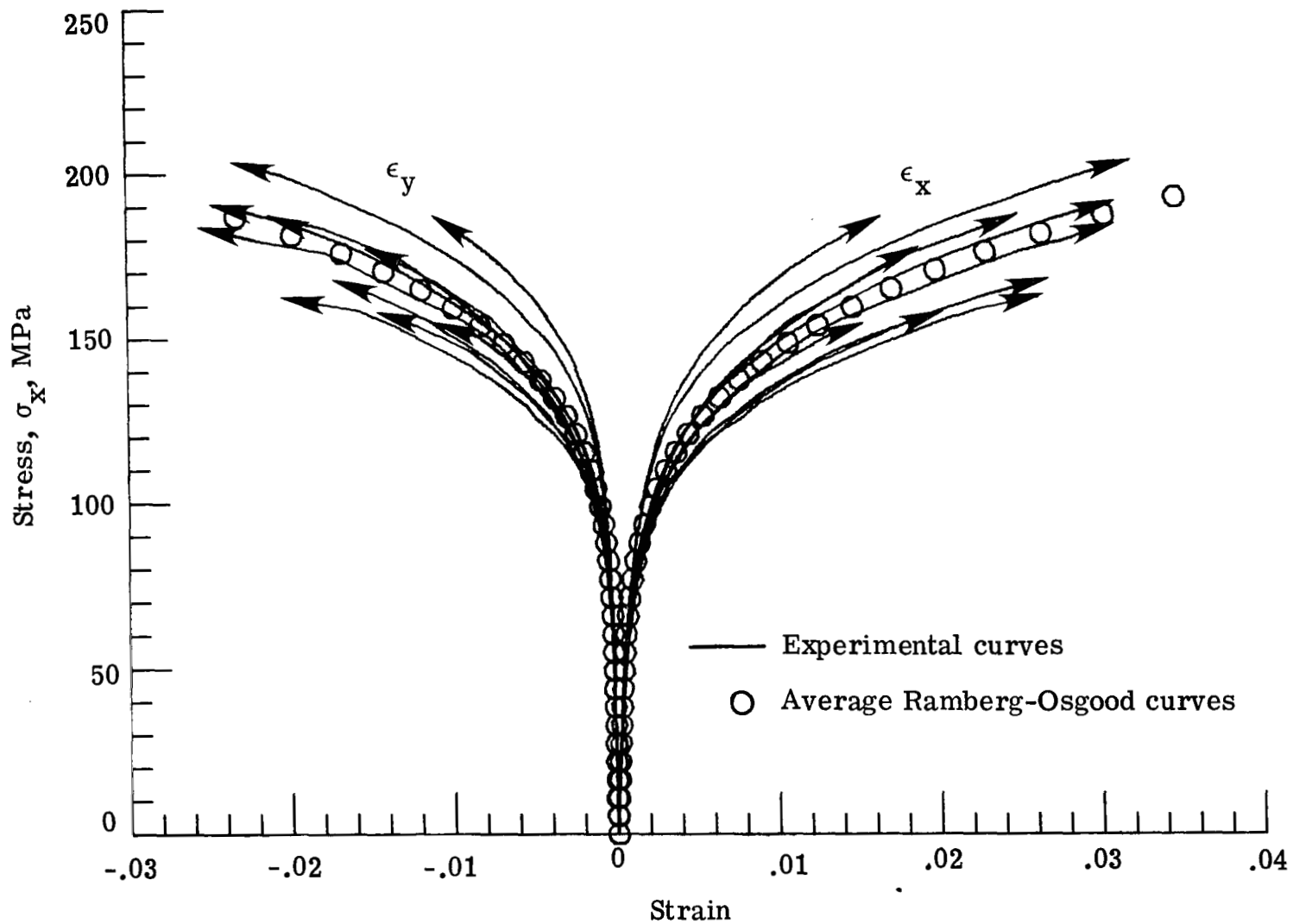
(b) Transverse tests.

Figure 7.- Concluded.



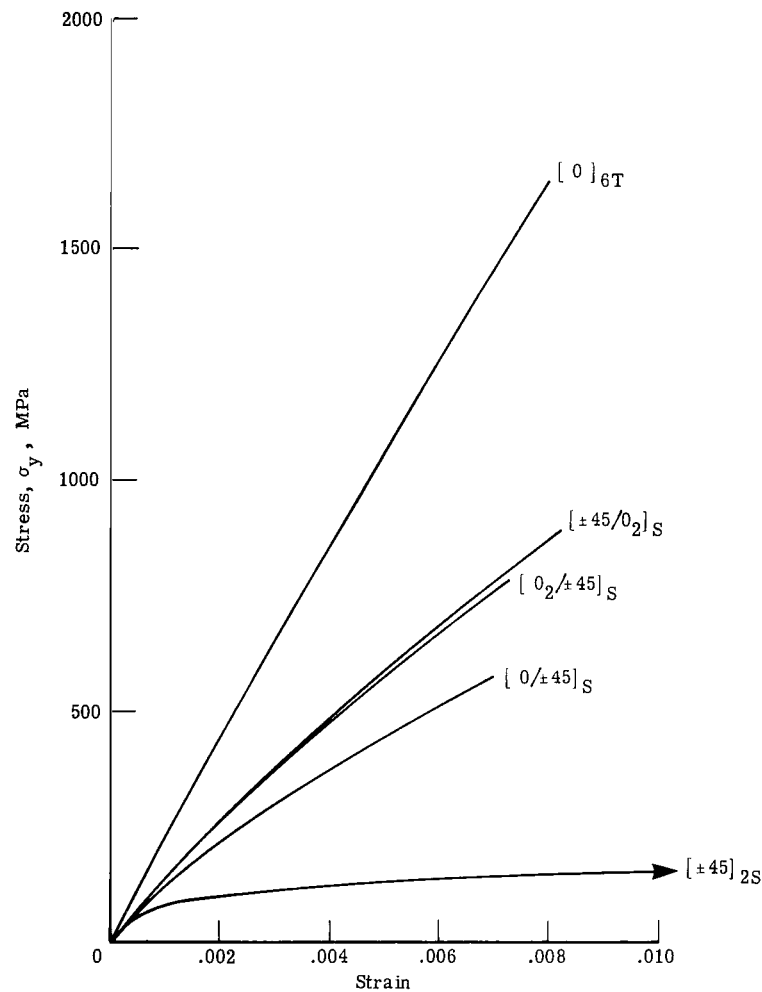
(a) Longitudinal tests.

Figure 8.- Stress-strain curves for $[+45]_{2S}$ laminates.

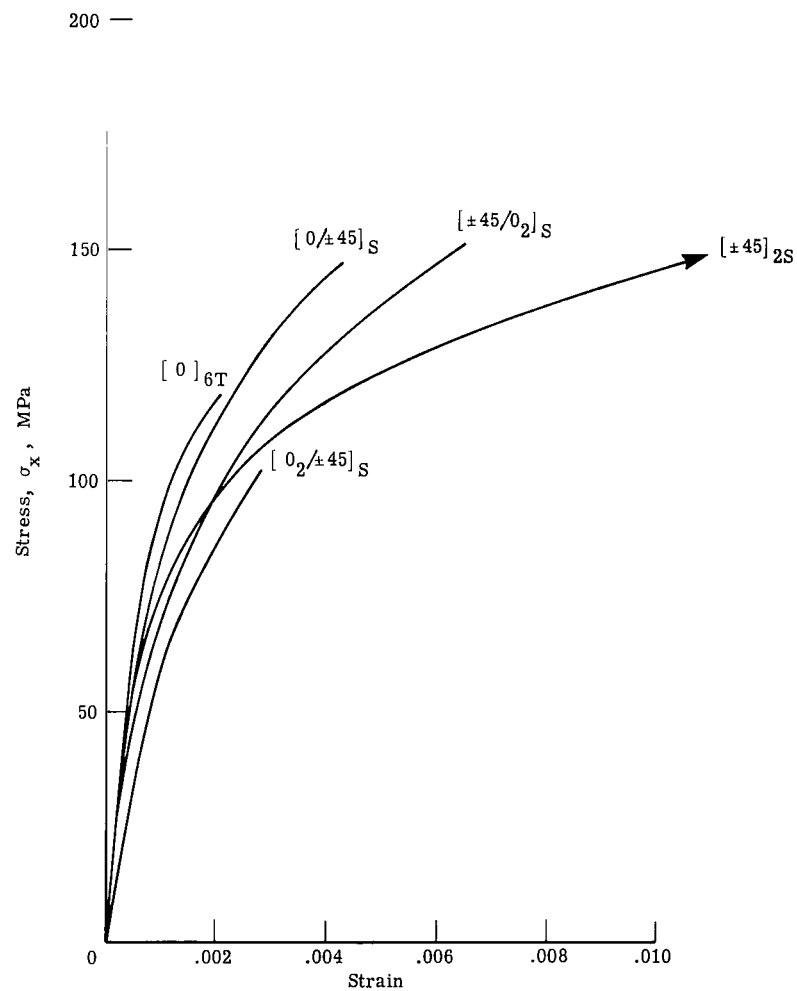


(b) Transverse tests.

Figure 8.- Concluded.

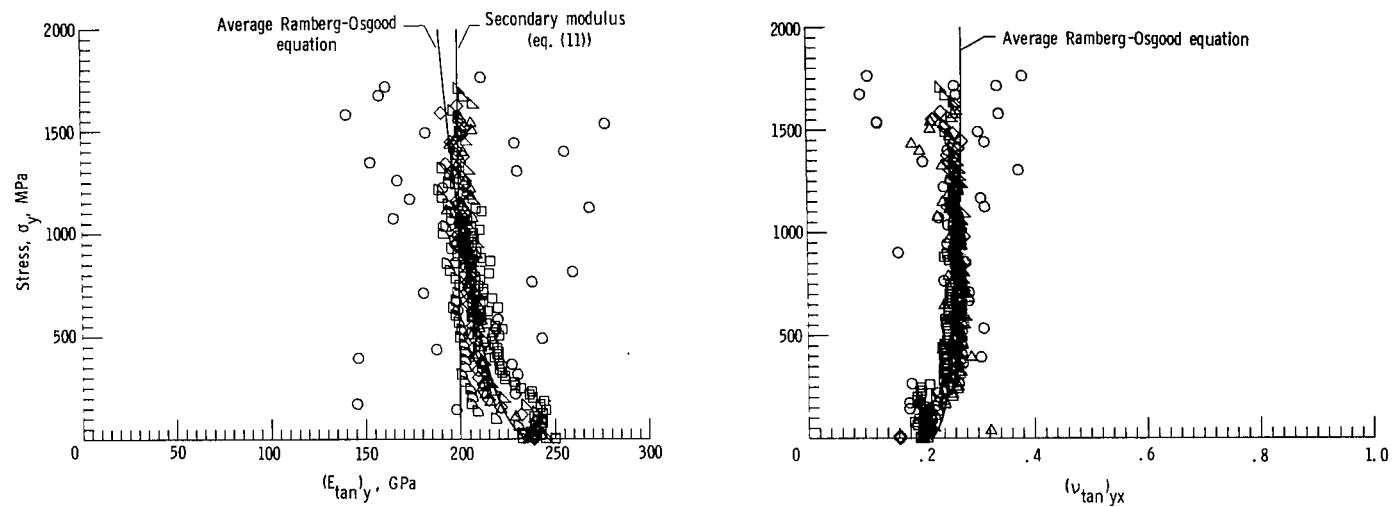


(a) Longitudinal tests.

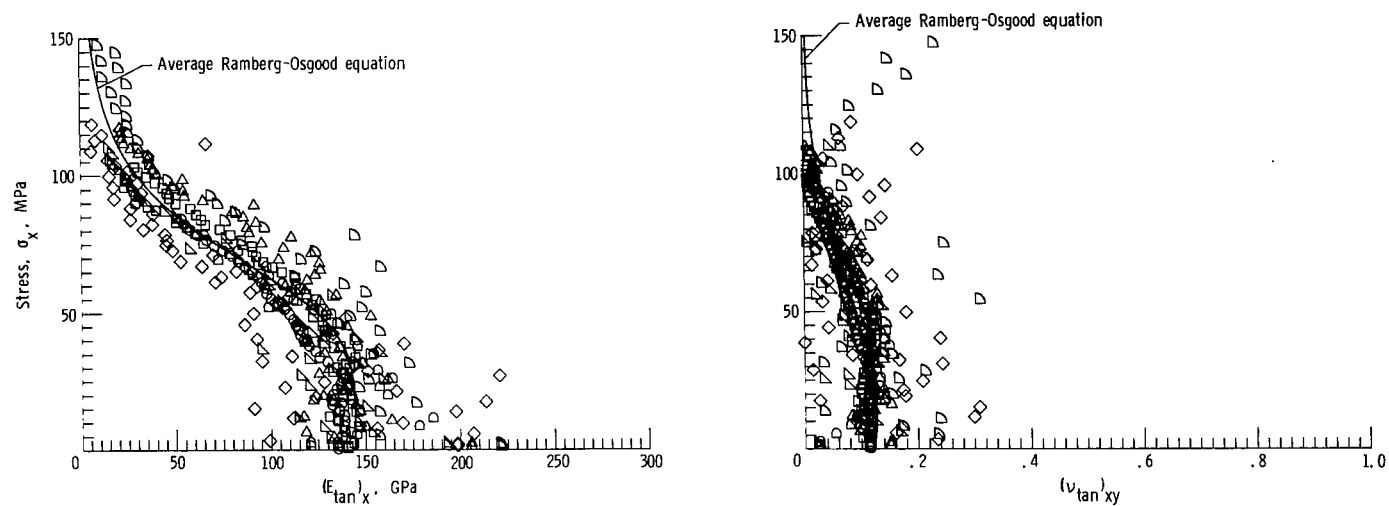


(b) Transverse tests.

Figure 9.- Average Ramberg-Osgood stress-strain curves for boron/aluminum laminates.

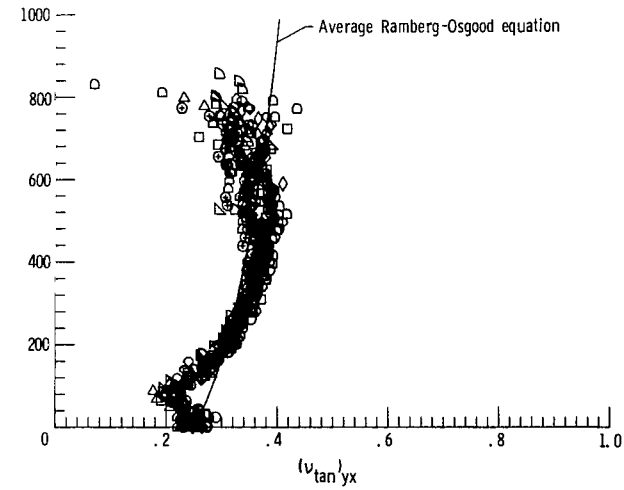
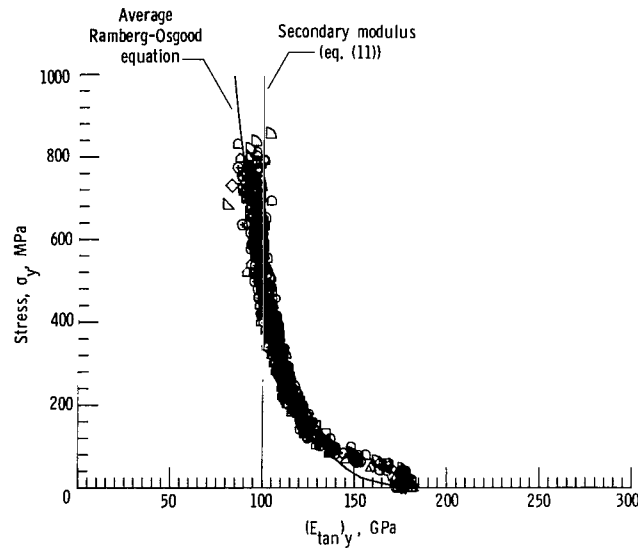


(a) Longitudinal tests.

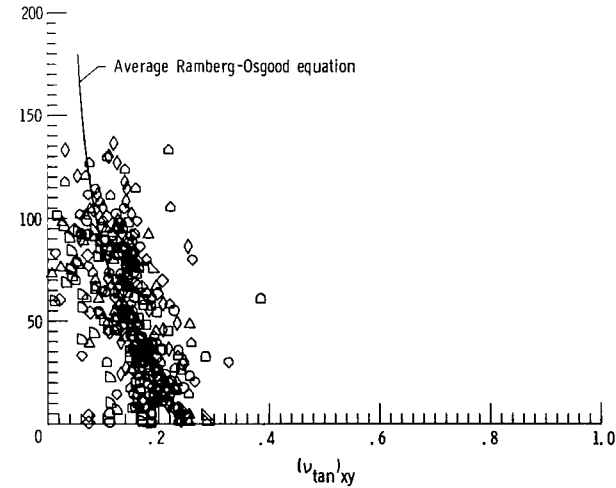
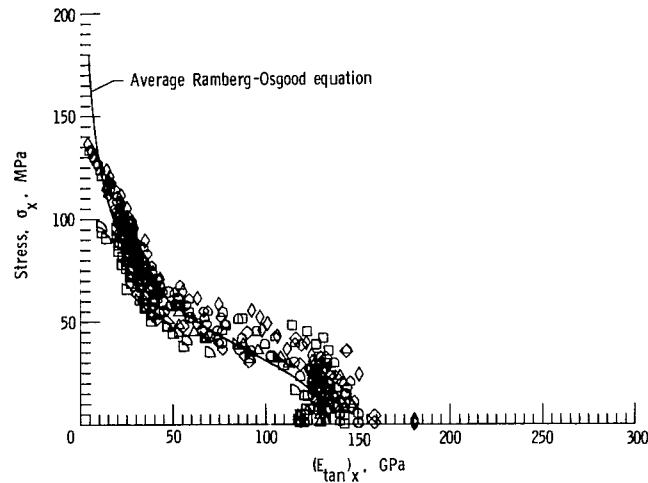


(b) Transverse tests.

Figure 10.- Tangent moduli and Poisson's ratios for $[0]_{6T}$ laminates.

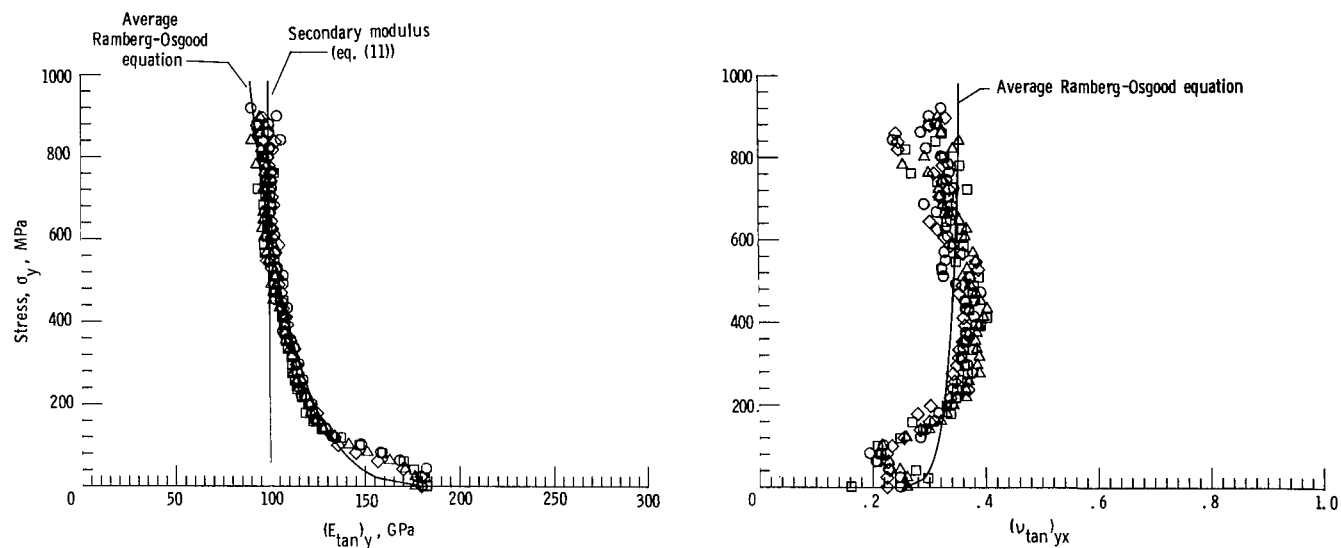


(a) Longitudinal tests.

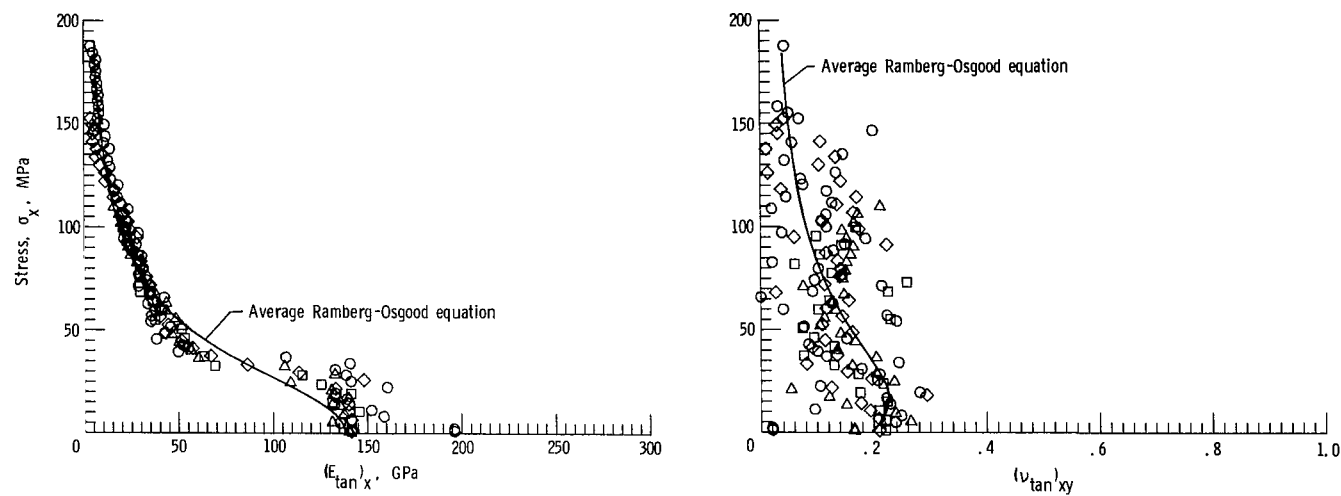


(b) Transverse tests.

Figure 11.- Tangent moduli and Poisson's ratios for $[0_2/\pm 45]_S$ laminates.

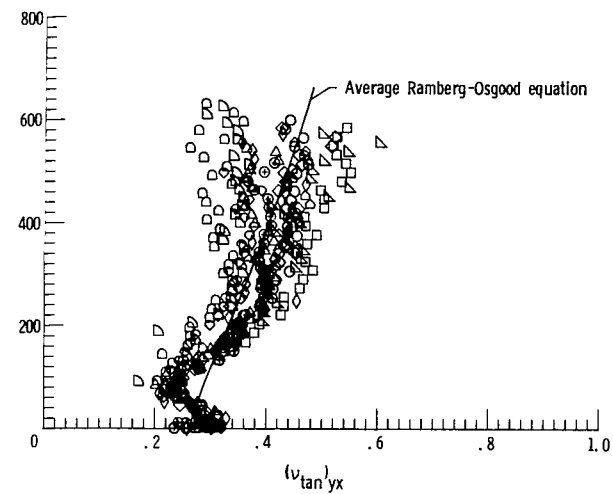
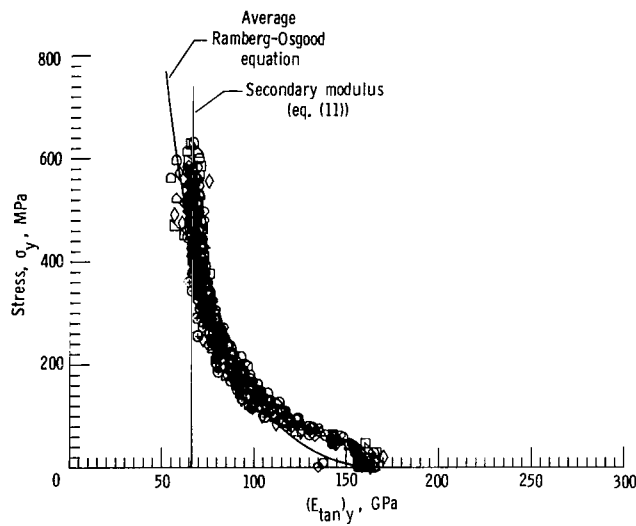


(a) Longitudinal tests.

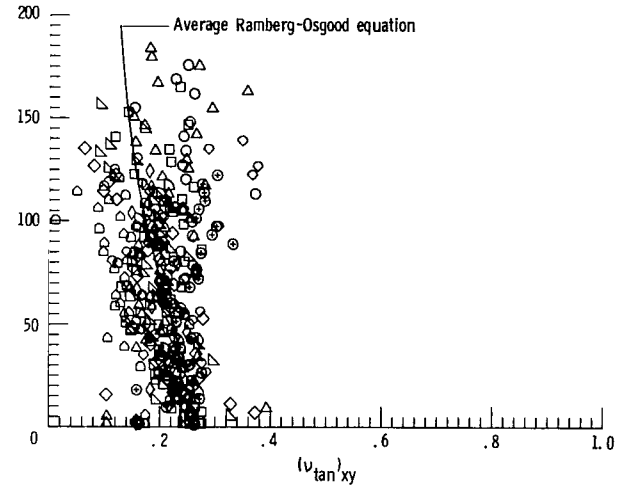
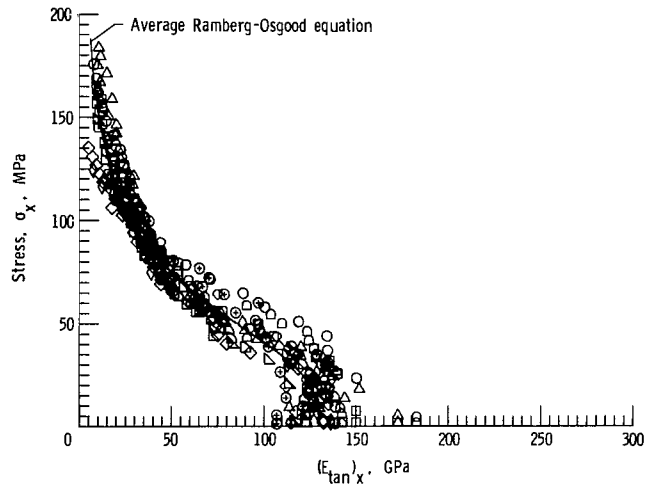


(b) Transverse tests.

Figure 12.- Tangent moduli and Poisson's ratios for $[\pm 45/0_2]_S$ laminates.

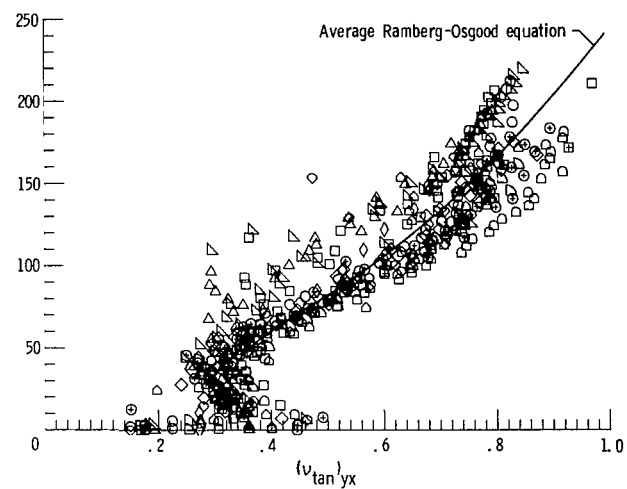
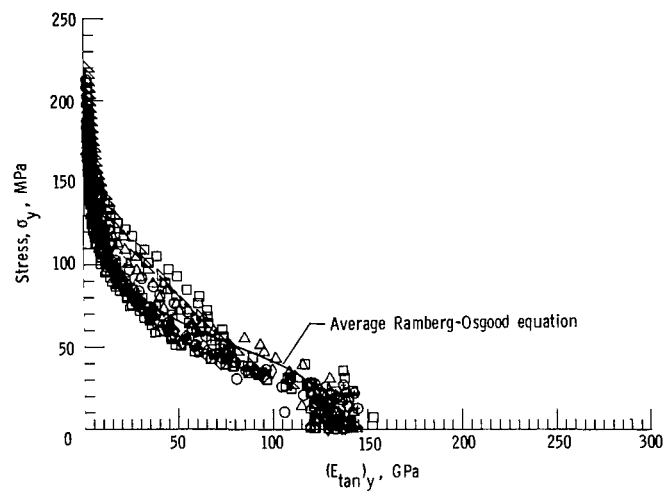


(a) Longitudinal tests.

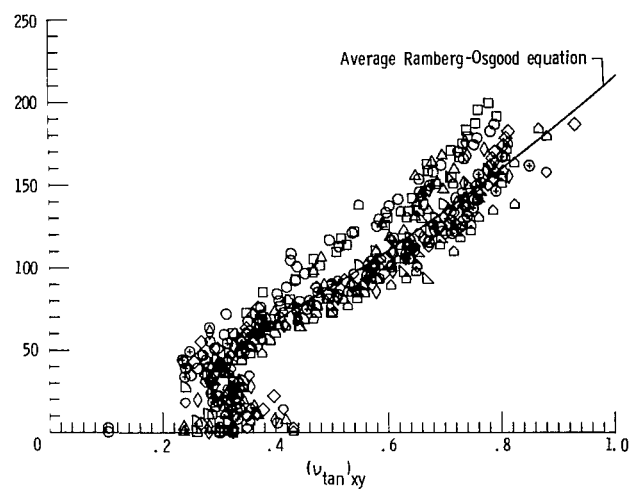
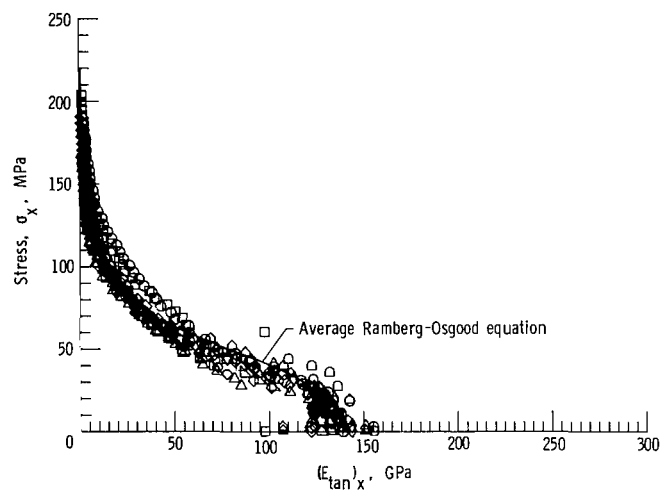


(b) Transverse tests.

Figure 13.- Tangent moduli and Poisson's ratios for $[0/\pm 45]_S$ laminates.

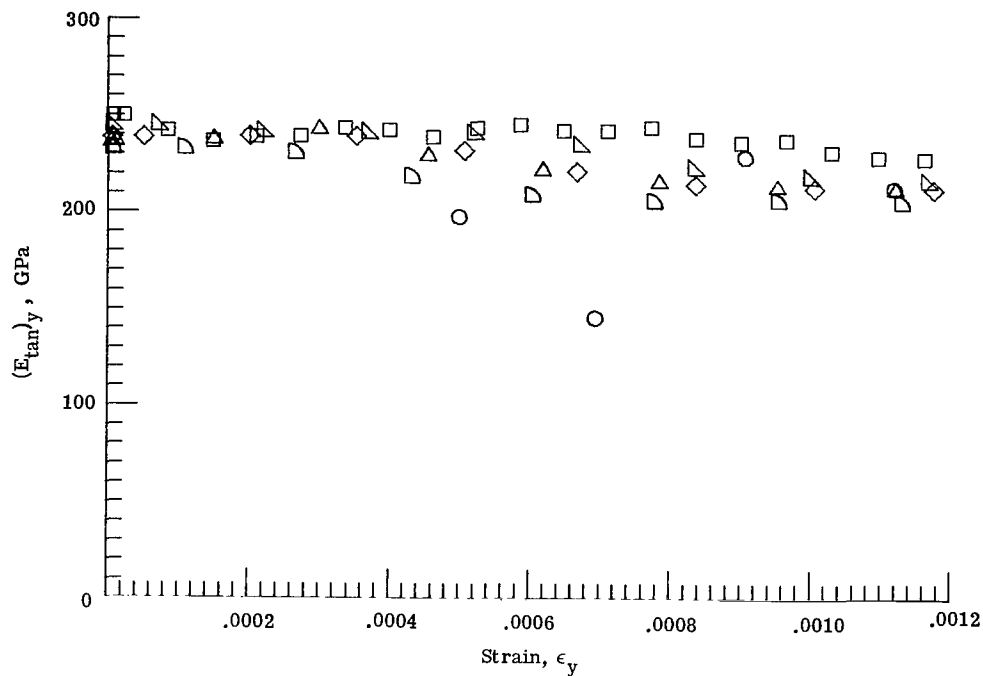


(a) Longitudinal tests.

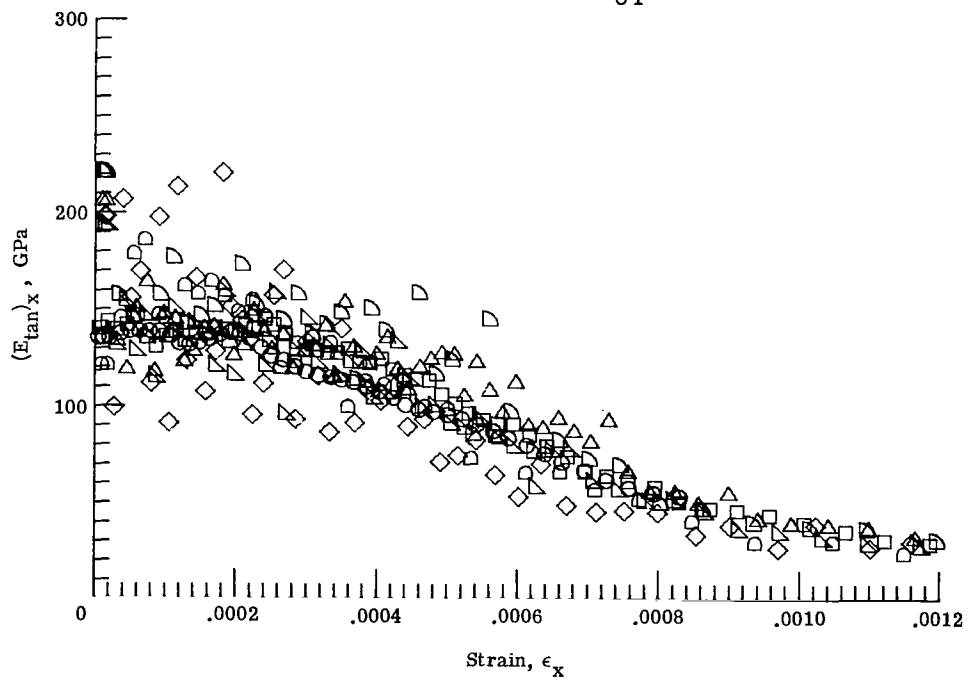


(b) Transverse tests.

Figure 14.- Tangent moduli and Poisson's ratios for $[\pm 45]_{2S}$ laminates.

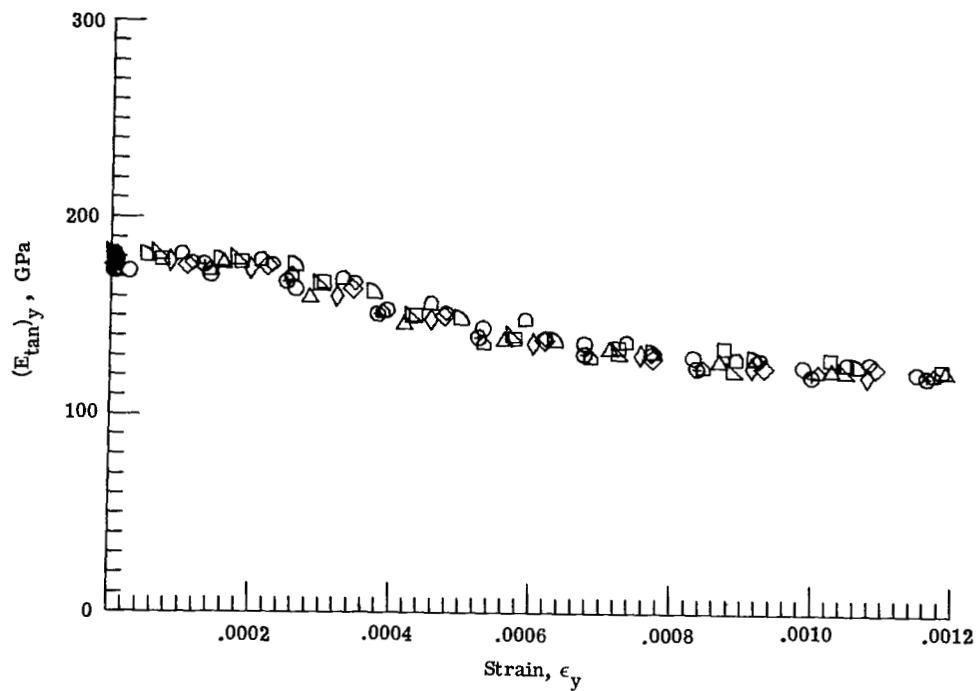


(a) Longitudinal tests of $[0]_{6T}$ laminates.

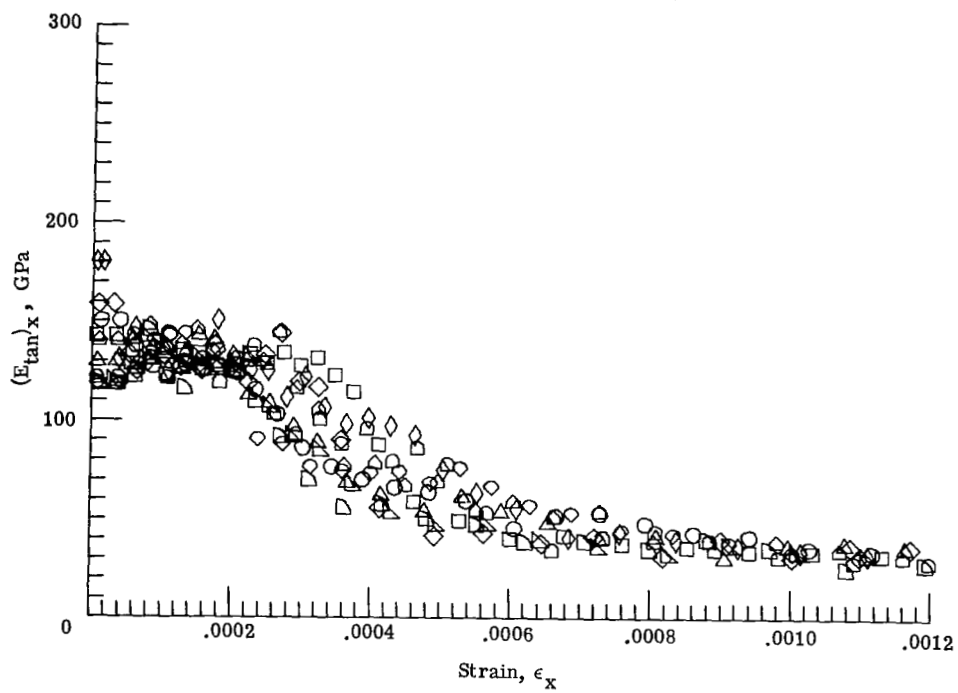


(b) Transverse tests of $[0]_{6T}$ laminates.

Figure 15.- Tangent moduli at small strains.

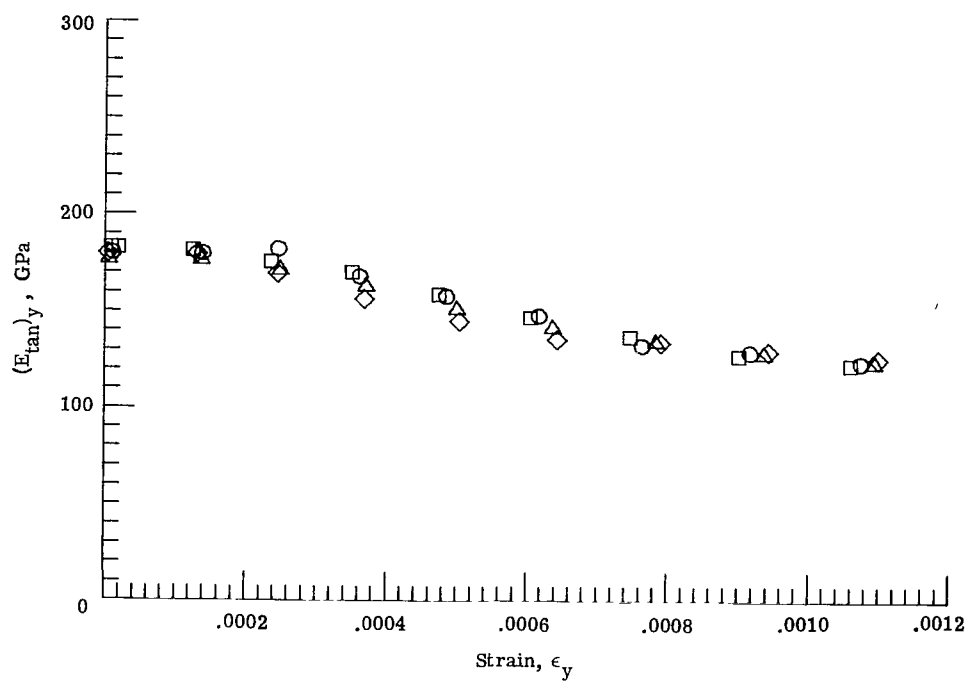


(c) Longitudinal tests of $[0_2/+45]_S$ laminates.

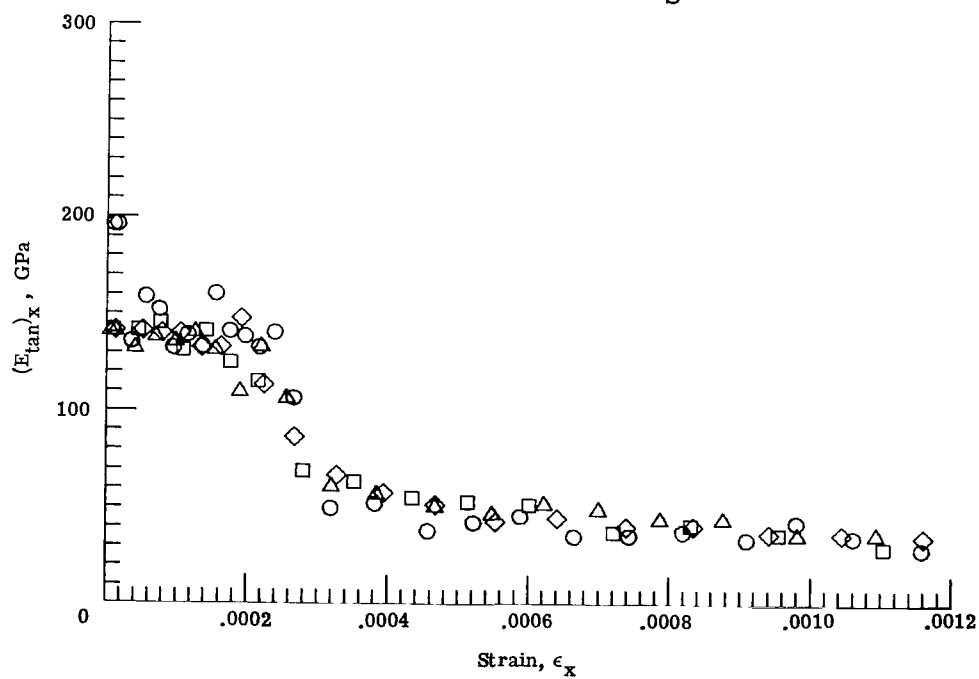


(d) Transverse tests of $[0_2/+45]_S$ laminates.

Figure 15.- Continued.

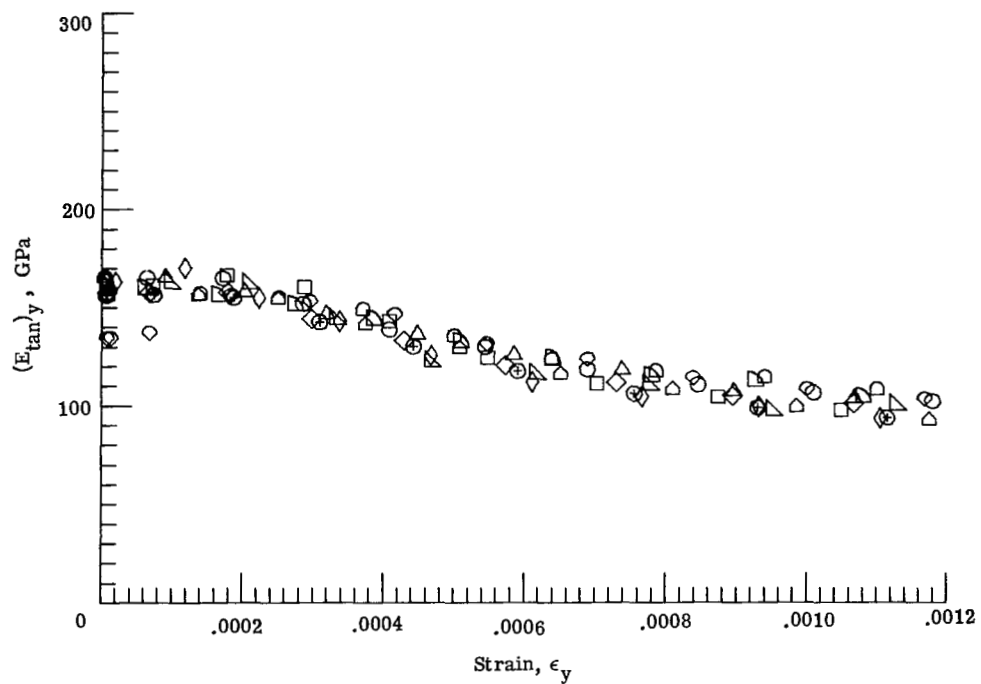


(e) Longitudinal tests of $[+45/0_2]_S$ laminates.

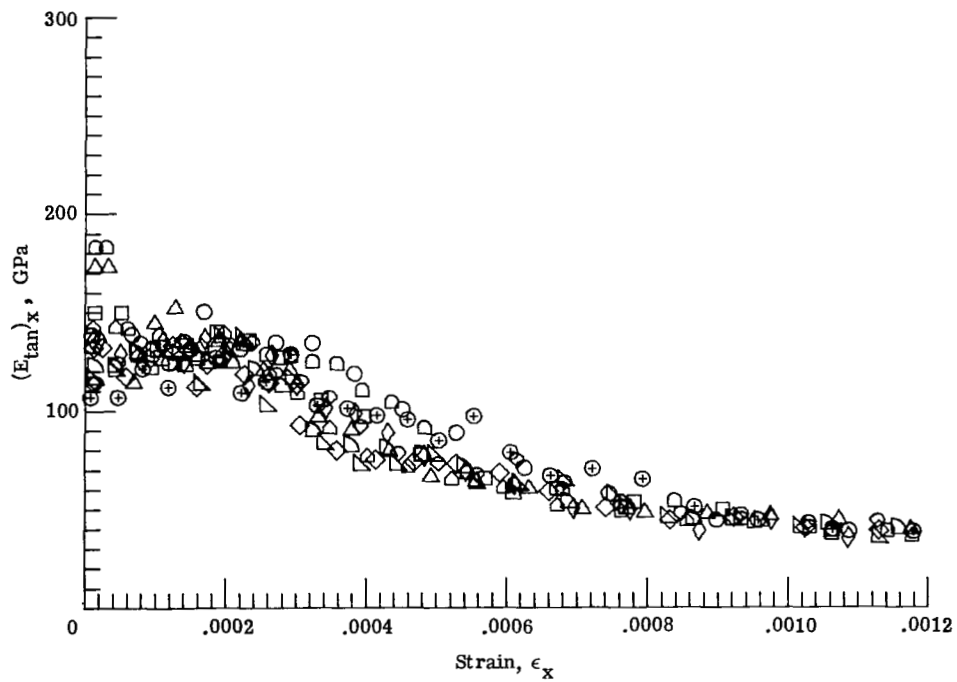


(f) Transverse tests of $[+45/0_2]_S$ laminates.

Figure 15.- Continued.

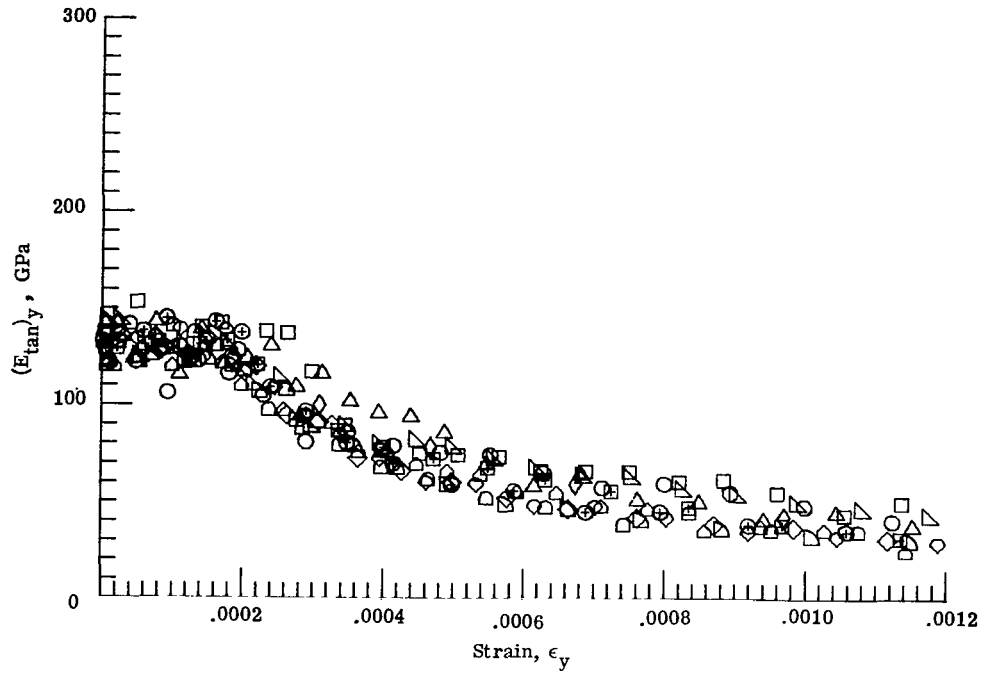


(g) Longitudinal tests of $[0/+45]_S$ laminates.

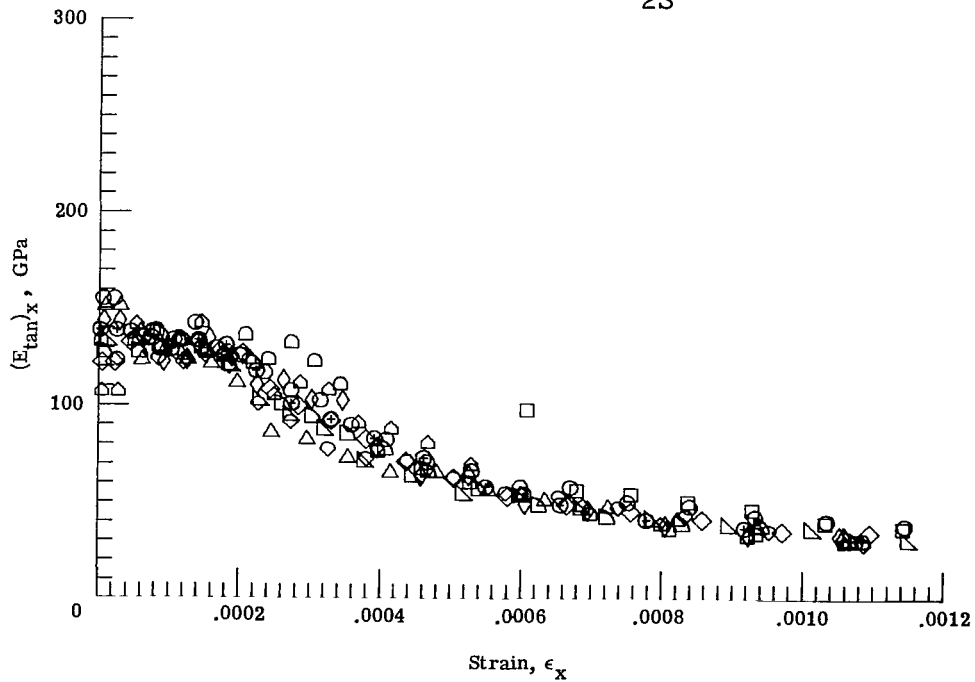


(h) Transverse tests of $[0/+45]_S$ laminates.

Figure 15.- Continued.



(i) Longitudinal tests of $[+45]_{2S}$ laminates.



(j) Transverse tests of $[+45]_{2S}$ laminates.

Figure 15.- Concluded.

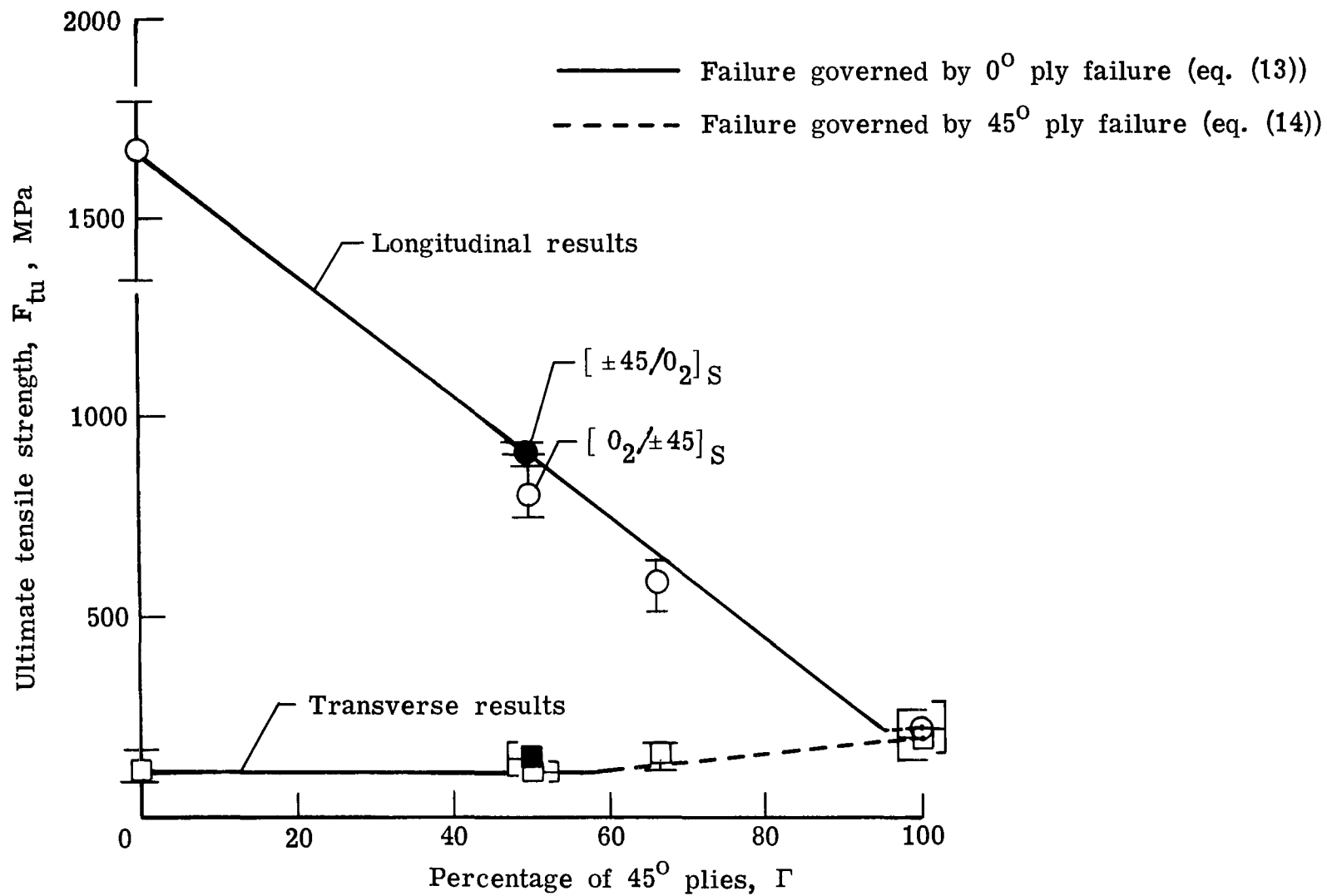
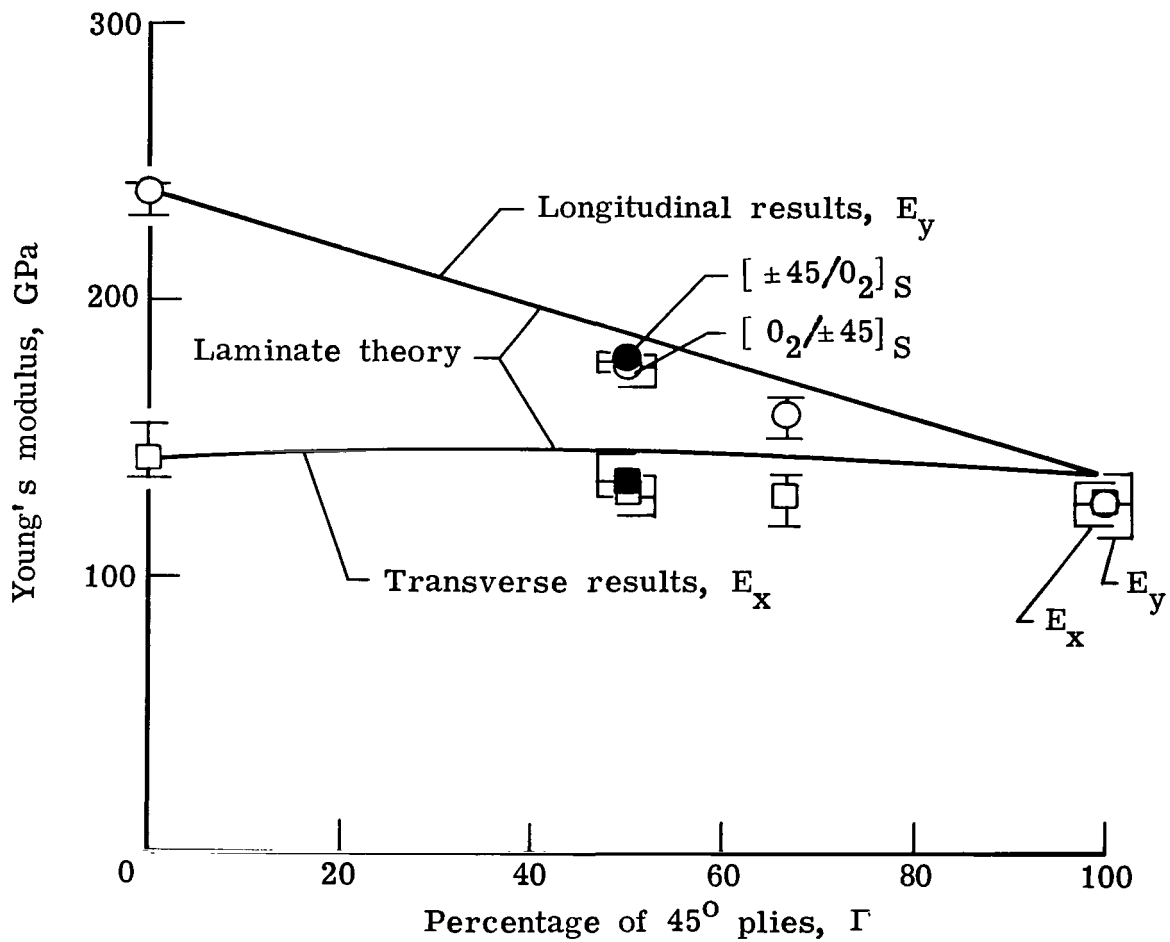
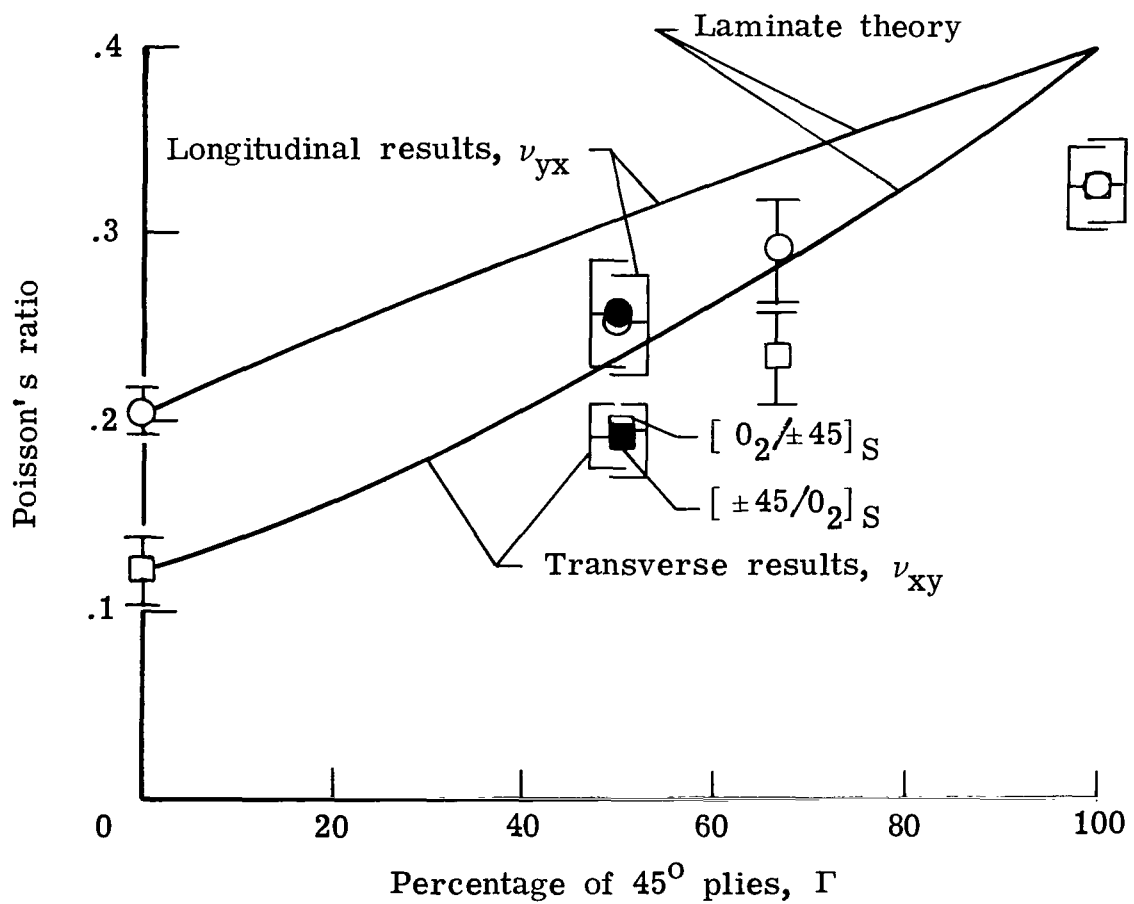


Figure 16.- Ultimate tensile strength for longitudinal and transverse tests.



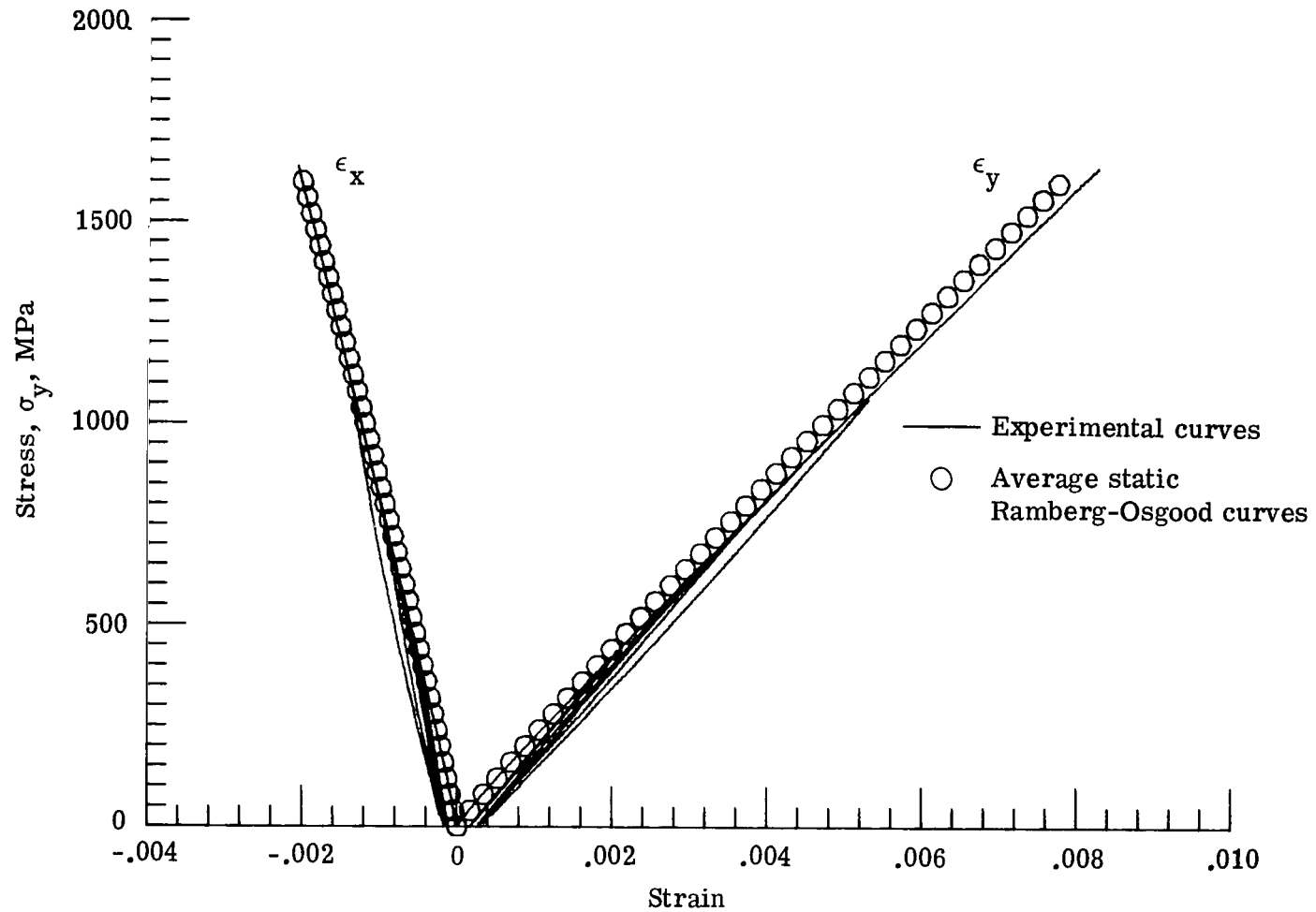
(a) Young's modulus.

Figure 17.- Elastic constants for longitudinal and transverse tests.



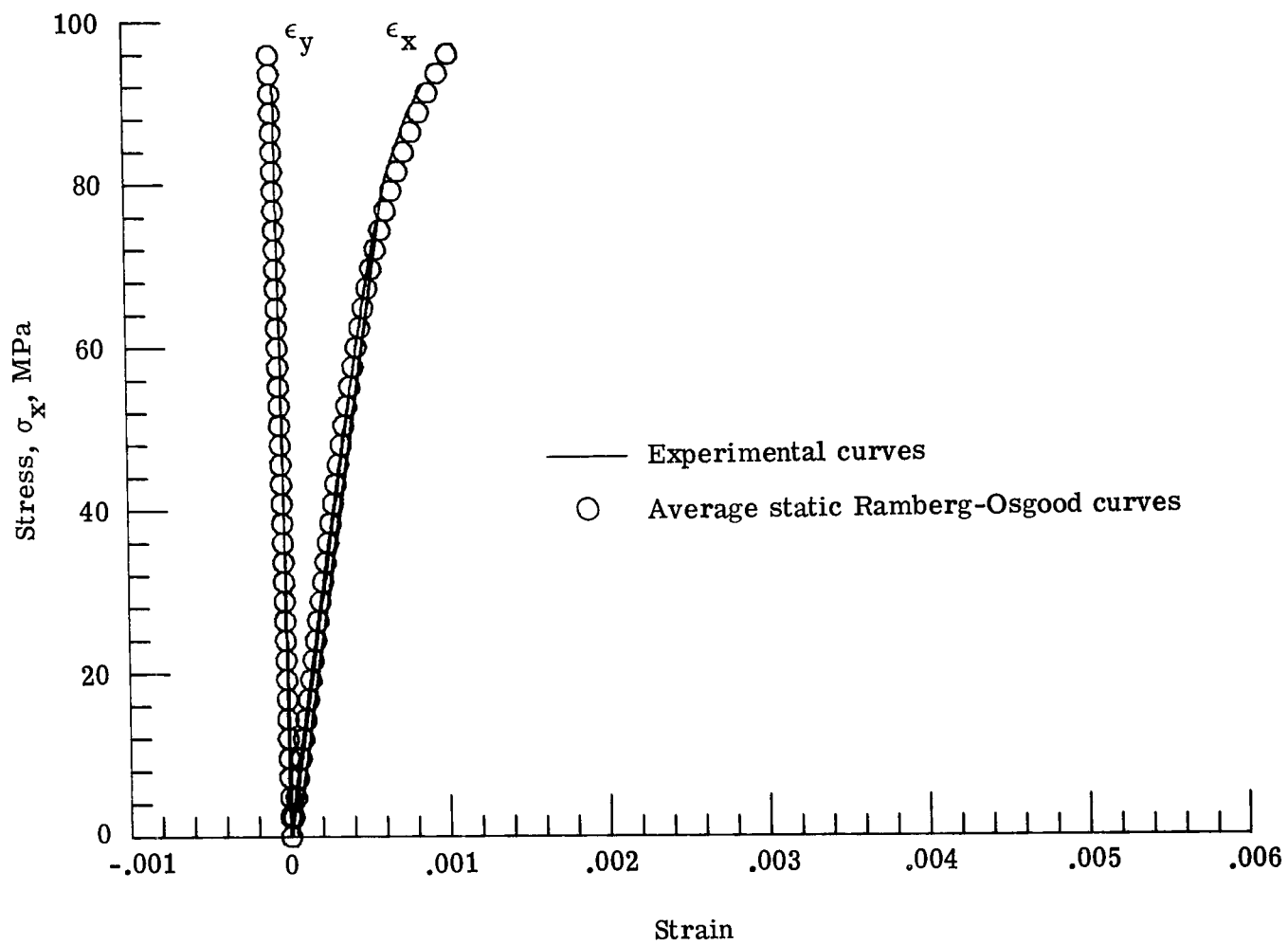
(b) Poisson's ratio.

Figure 17.- Concluded.



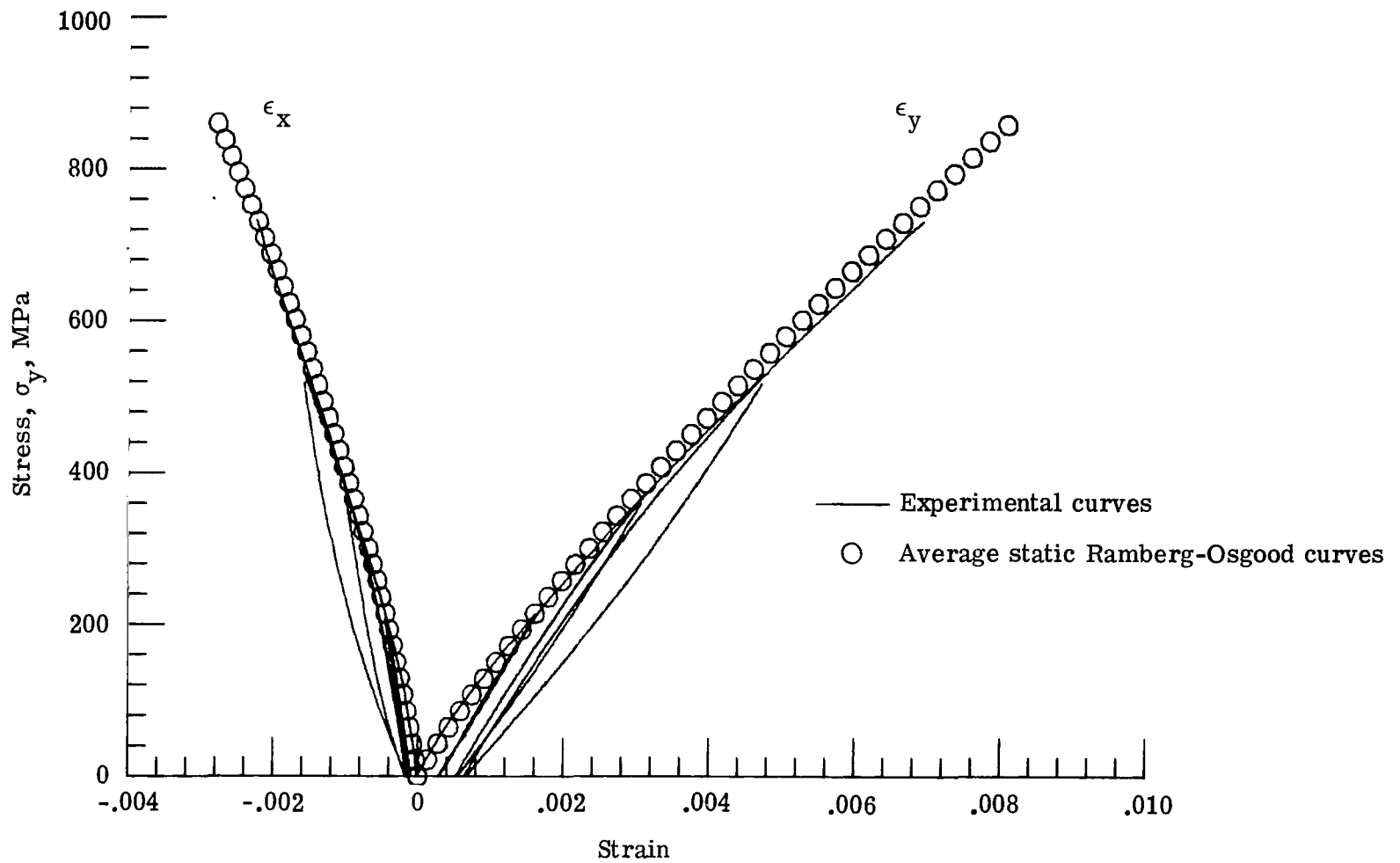
(a) Longitudinal test.

Figure 18.- Stress-strain curve for $[0]_{6T}$ laminate subjected to three loading cycles.



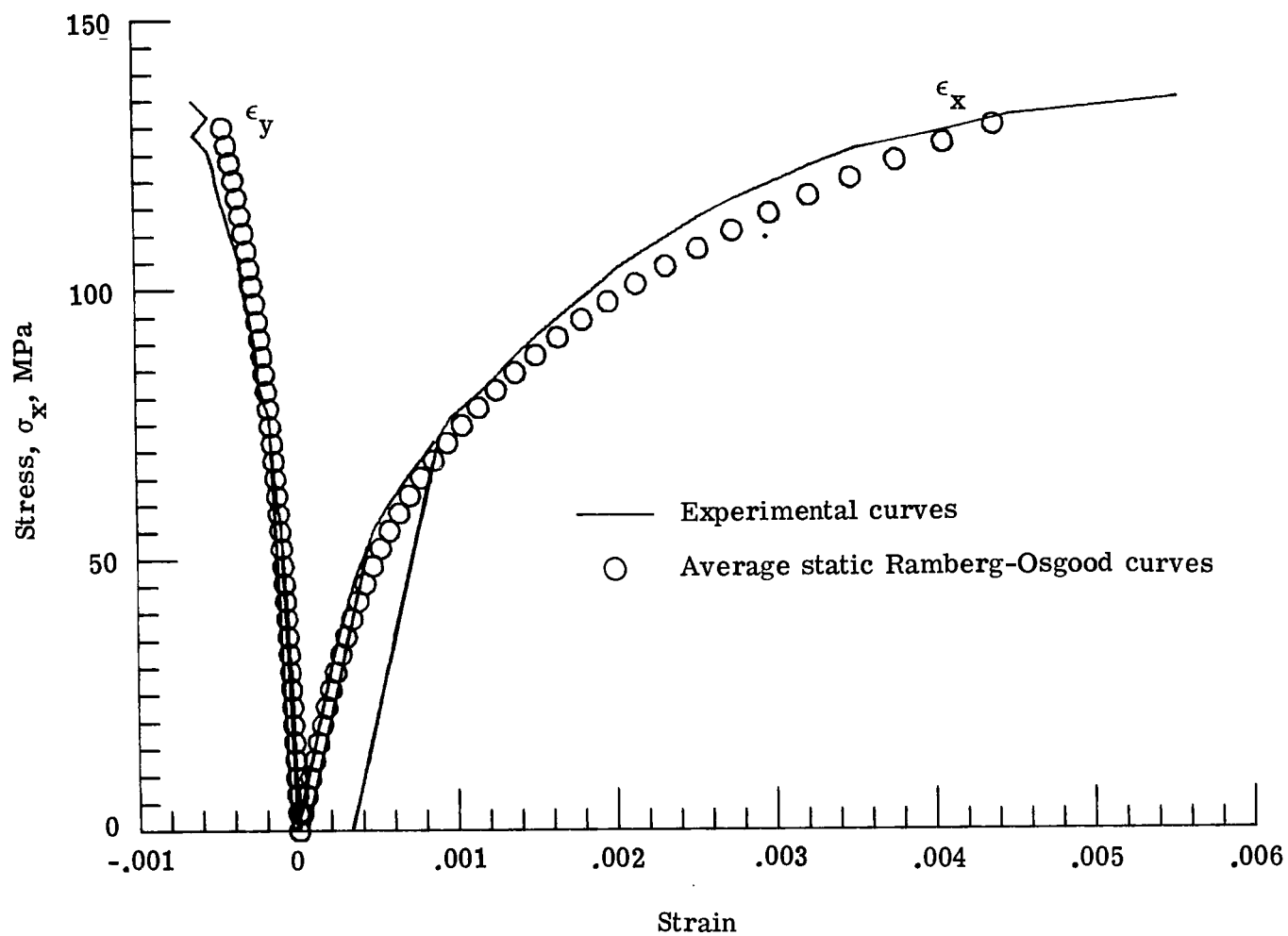
(b) Transverse test.

Figure 18.- Concluded.



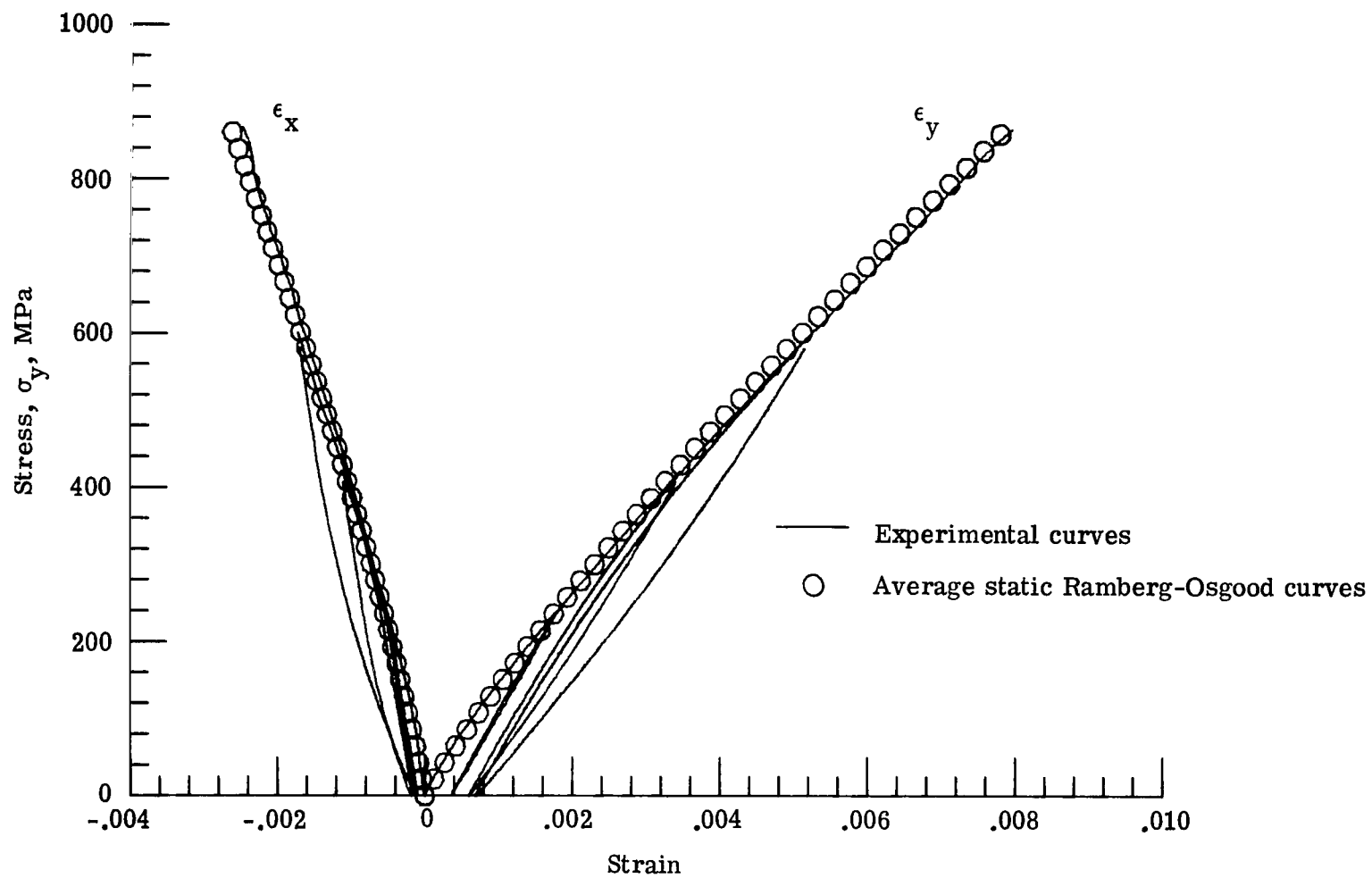
(a) Longitudinal test.

Figure 19.- Stress-strain curve for $[0_2/+45]_S$ laminate subjected to three loading cycles.



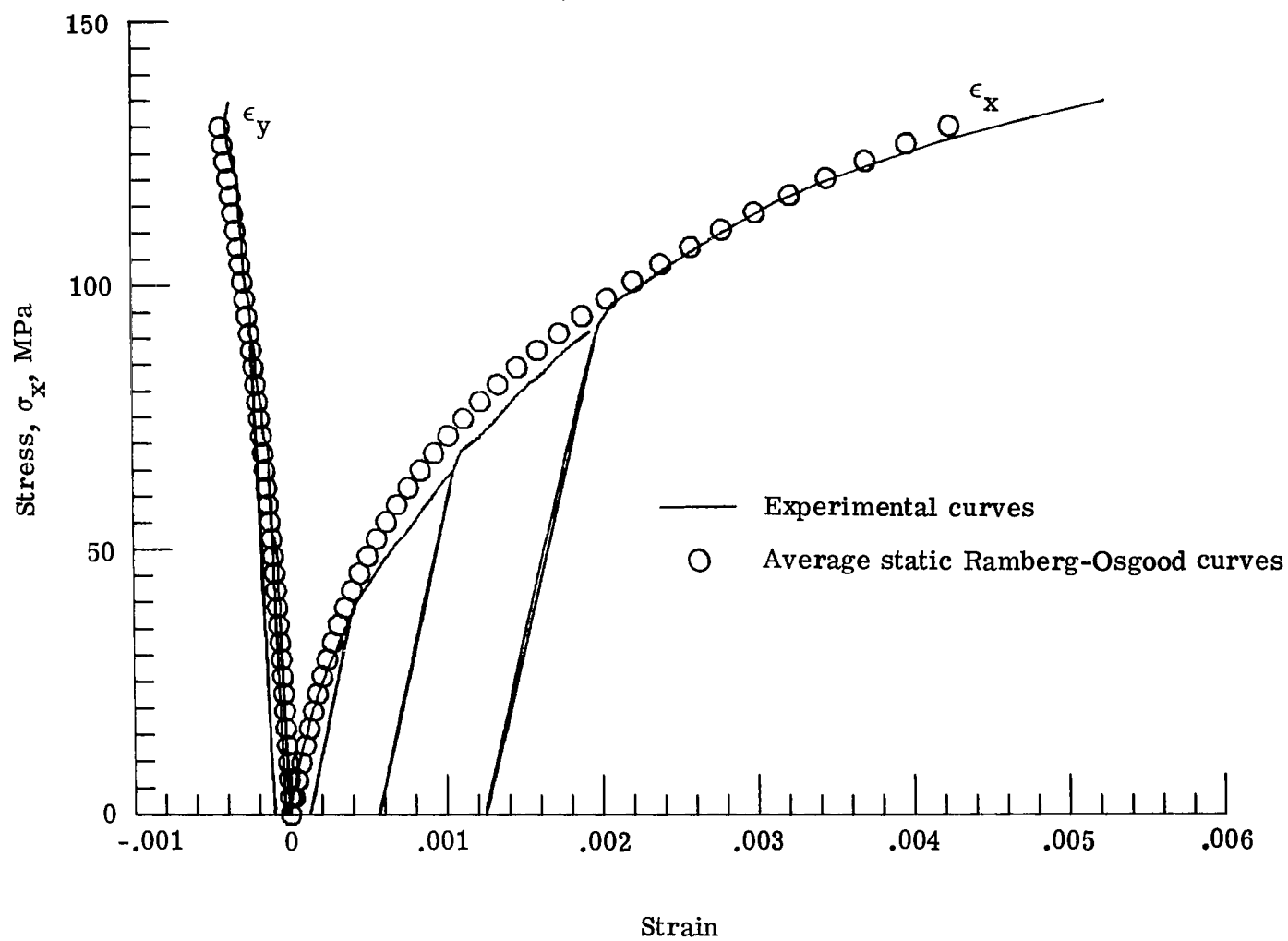
(b) Transverse test.

Figure 19.- Concluded.



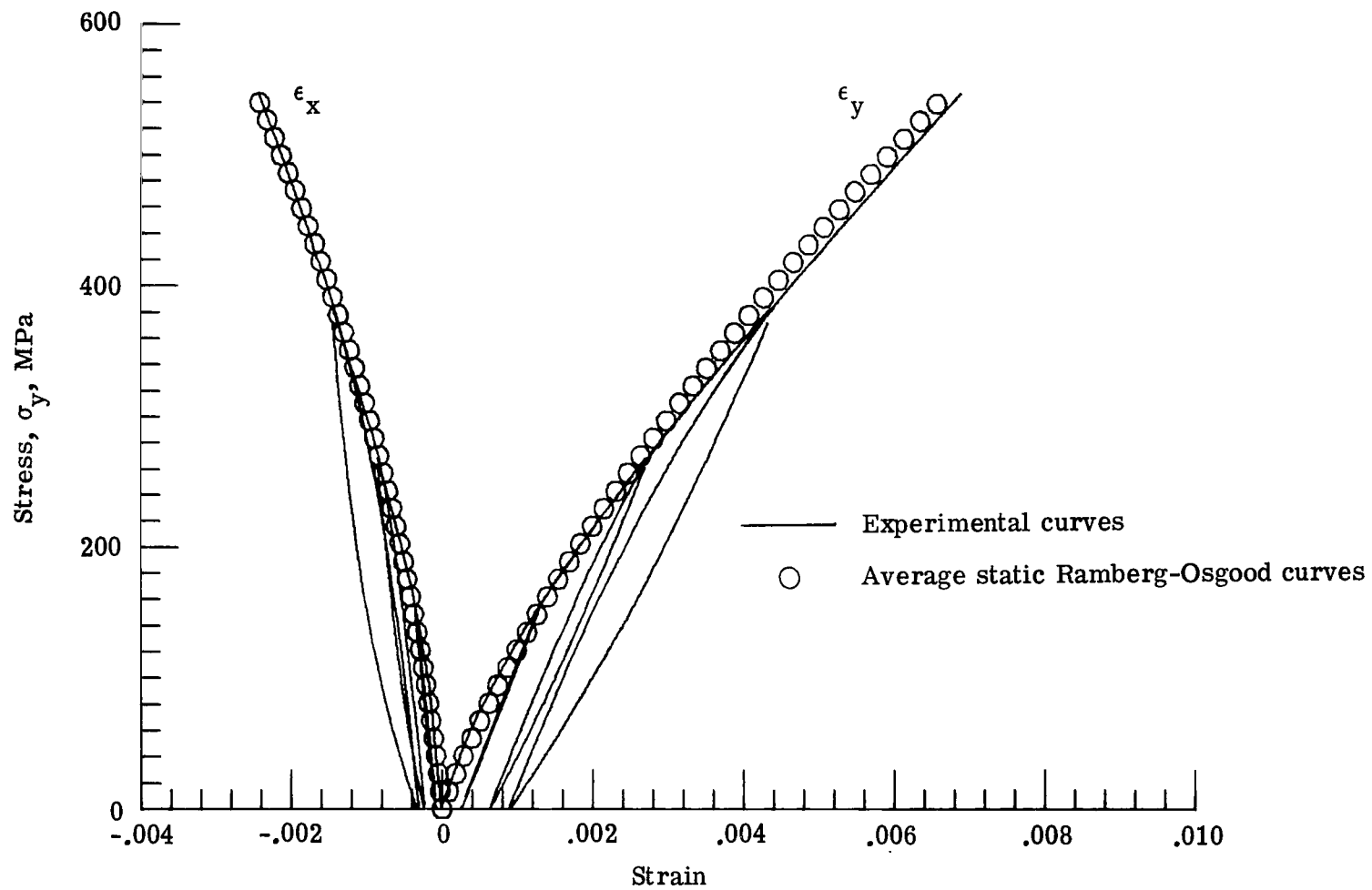
(a) Longitudinal test.

Figure 20.- Stress-strain curve for $[\pm 45/0_2]_S$ laminate subjected to three loading cycles.



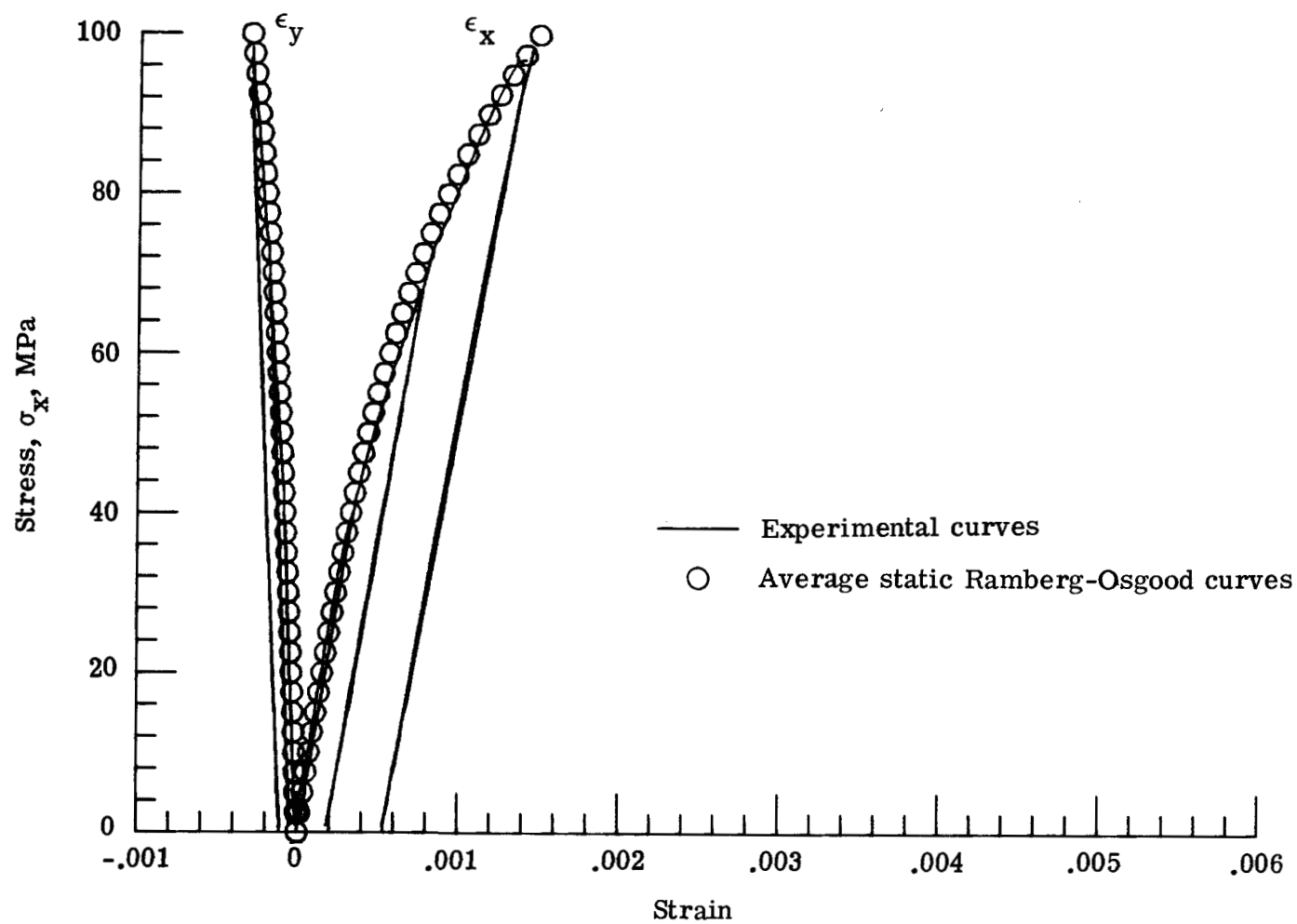
(b) Transverse test.

Figure 20.- Concluded.



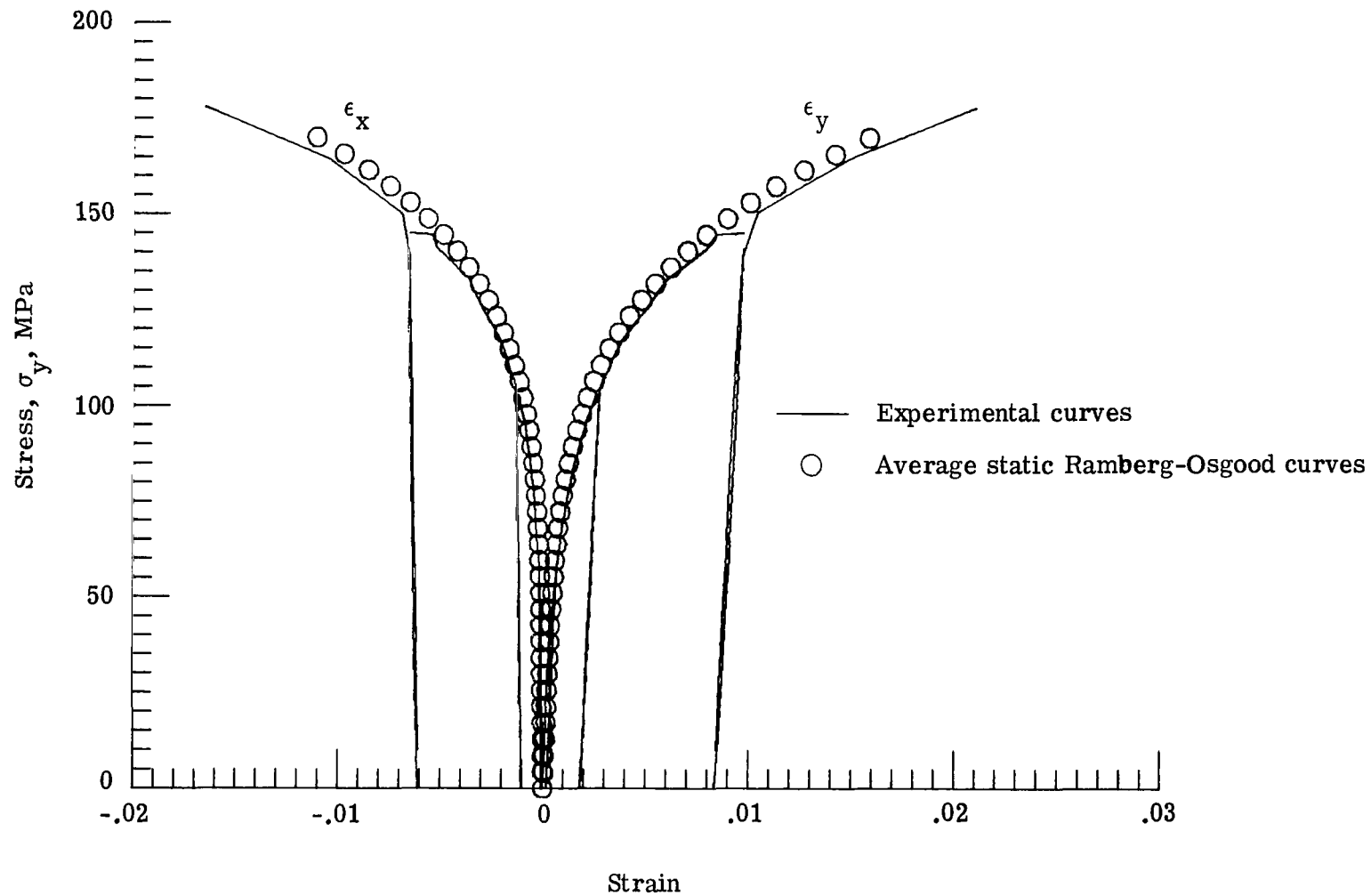
(a) Longitudinal test.

Figure 21.- Stress-strain curve for $[0/+45]_S$ laminate subjected to three loading cycles.



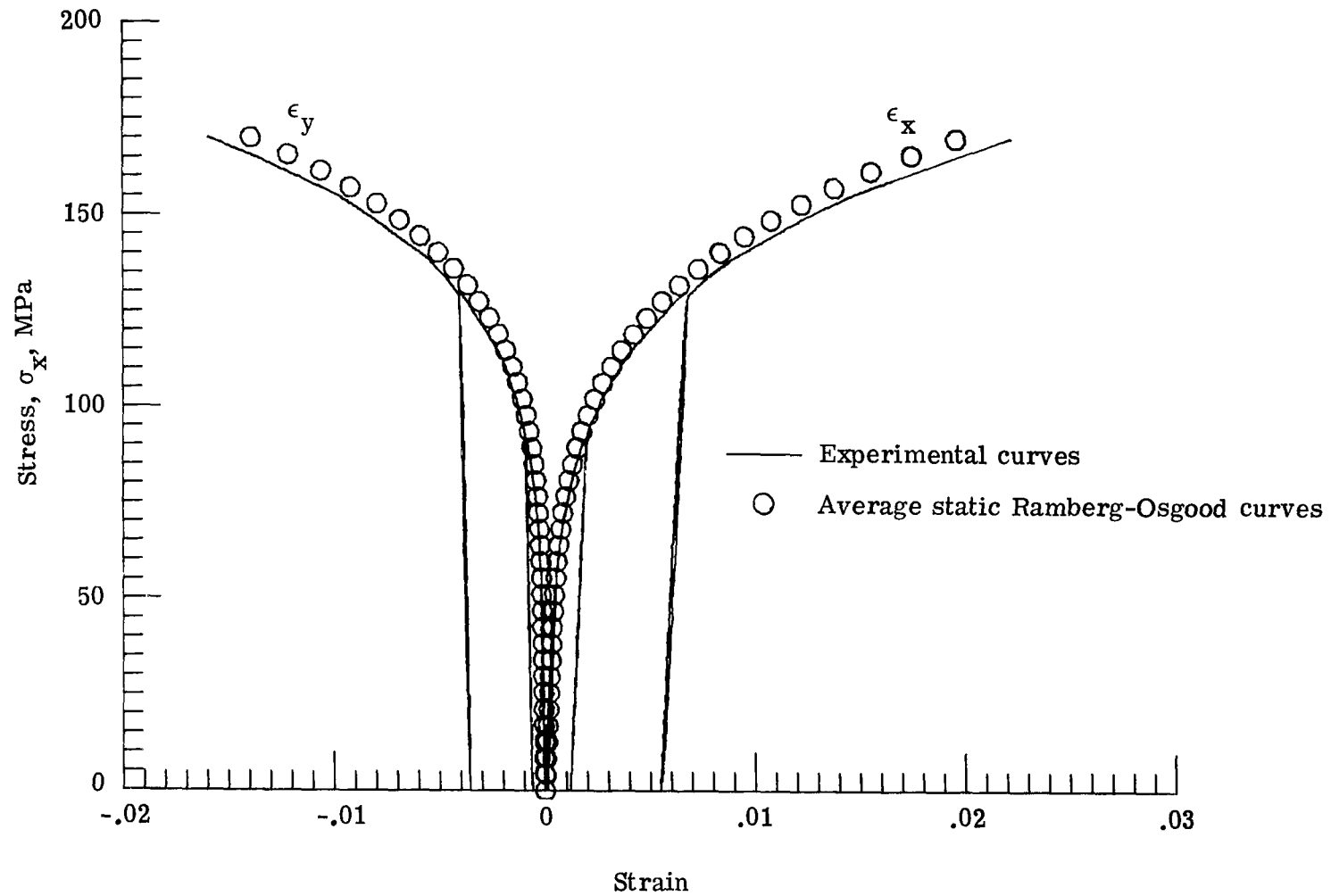
(b) Transverse test.

Figure 21.- Concluded.



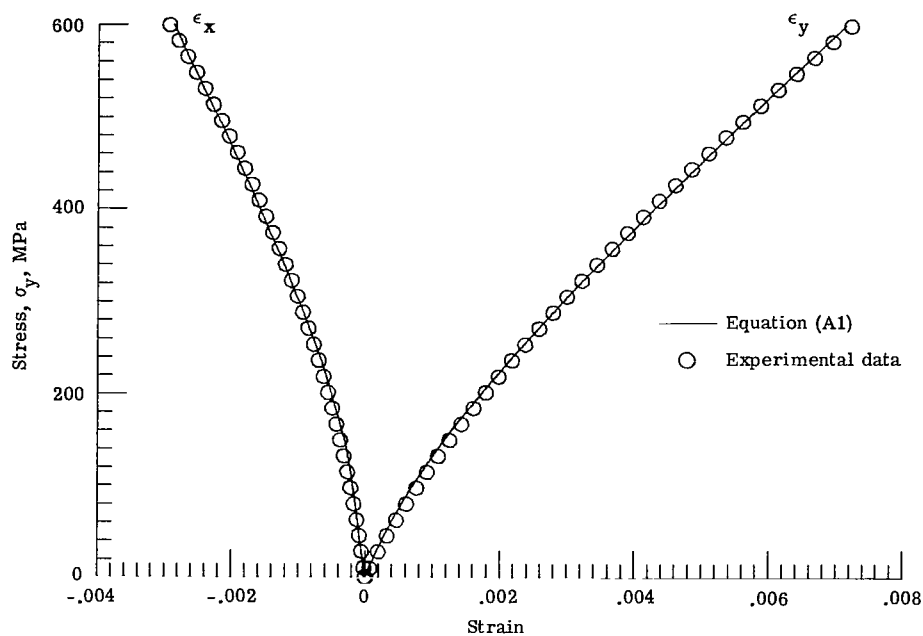
(a) Longitudinal test.

Figure 22.- Stress-strain curve for $[\pm 45]_{2S}$ laminate subjected to three loading cycles.

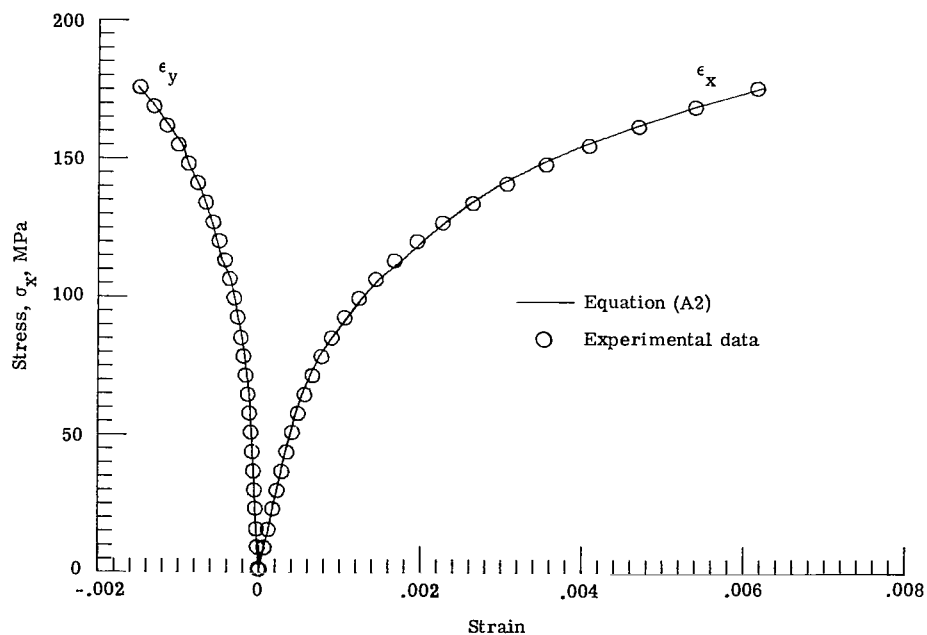


(b) Transverse test.

Figure 22.- Concluded.



(a) Longitudinal test (specimen no. 2628).



(b) Transverse test (specimen no. 2629).

Figure 23.- Fit of Ramberg-Osgood equation to stress-strain data for a $[0/\pm 45]_S$ specimen.

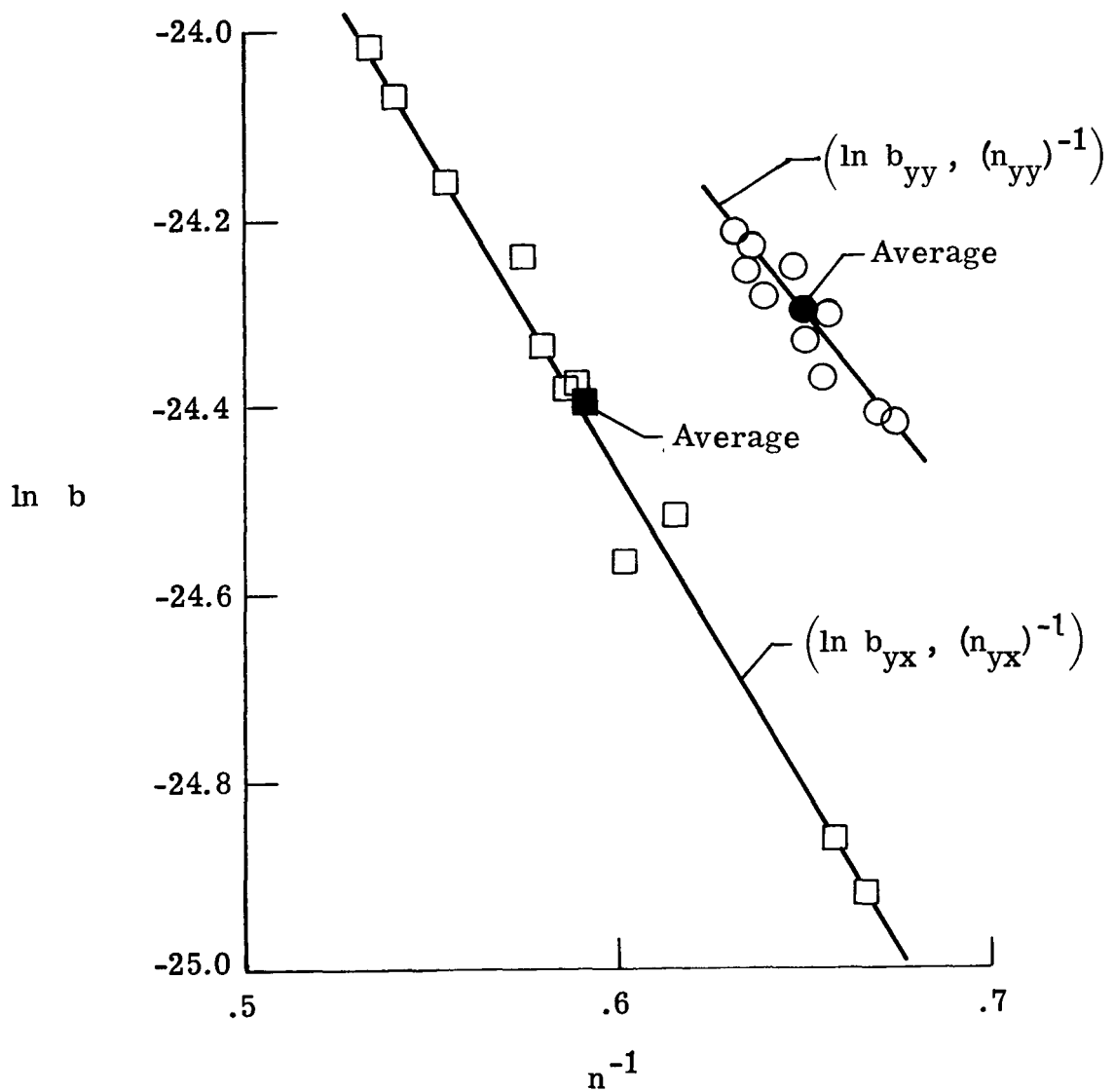


Figure 24.- Ramberg-Osgood constants for longitudinal tests of $[0_2/\pm 45]_S$ laminates.

1. Report No. NASA TP-1117		2. Government Accession No.		3. Recipient's Catalog No.	
4. Title and Subtitle TENSILE STRESS-STRAIN BEHAVIOR OF BORON/ALUMINUM LAMINATES				5. Report Date February 1978	
				6. Performing Organization Code	
7. Author(s) J. A. Sova and C. C. Poe, Jr.				8. Performing Organization Report No. L-11864	
9. Performing Organization Name and Address NASA Langley Research Center Hampton, VA 23665				10. Work Unit No. 743-01-01-04	
				11. Contract or Grant No.	
12. Sponsoring Agency Name and Address National Aeronautics and Space Administration Washington, DC 20546				13. Type of Report and Period Covered Technical Paper	
				14. Sponsoring Agency Code	
15. Supplementary Notes J. A. Sova: Joint Institute for Advancement of Flight Sciences, The George Washington University, Hampton, Virginia. C. C. Poe, Jr.: Langley Research Center.					
16. Abstract <p>The tensile stress-strain behavior of five types of boron/aluminum laminates was investigated. Two of the laminate types contain only 0° or 45° fibers ($[0]_{6T}$ and $[+45]_{2S}$); the remaining three consisted of both 0° and 45° plies ($[0/+45]_S$, $[0_2/+45]_S$, and $[+45/0_2]_S$). Longitudinal and transverse stress-strain curves were obtained for monotonic loading to failure and for three cycles of loading to successively higher load levels.</p> <p>The laminate strengths predicted by assuming that the 0° plies failed first correlated well with the experimental results. The stress-strain curves for all the boron/aluminum laminates were nonlinear except at very small strains. Within the small linear regions, elastic constants calculated from laminate theory corresponded to those obtained experimentally to within 10 to 20 percent. A limited amount of cyclic loading did not affect the ultimate strength and strain for the boron/aluminum laminates. The laminates, however, exhibited a permanent strain on unloading.</p> <p>The Ramberg-Osgood equation was fitted to the stress-strain curves to obtain average curves for the various laminates. The equation fitted the experimental data well.</p>					
17. Key Words (Suggested by Author(s)) Five boron/aluminum laminates Tensile static and cyclic loading Ramberg-Osgood equation Strength prediction Nonlinearity Stress-strain curves			18. Distribution Statement Unclassified - Unlimited Subject Category 24		
19. Security Classif. (of this report) Unclassified	20. Security Classif. (of this page) Unclassified	21. No. of Pages 62	22. Price* \$5.25		

National Aeronautics and
Space Administration

Washington, D.C.
20546

Official Business

Penalty for Private Use, \$300

THIRD-CLASS BULK RATE

Postage and Fees Paid
National Aeronautics and
Space Administration
NASA-451



6 1 10, C. 012378 S00903DS
DEPT OF THE AIR FORCE
AF WEAPONS LABORATORY
ATTN: TECHNICAL LIBRARY (SUL)
KIRTLAND AFB NM 87117

NASA

POSTMASTER: If Undeliverable (Section 158
Postal Manual) Do Not Return

S